The APOBEC3G Deamination Independent Mode of HIV Inhibition

A Thesis Submitted to the

College of Graduate Studies and Research

in Partial Fulfillment of the Requirements for the

Degree of Master of Science in the

Department of Microbiology and Immunology

University of Saskatchewan

Saskatoon, SK

By

Jonathon Webb

PERMISSION TO USE

In presenting this thesis in partial fulfillment of the requirements for a Master of Science degree from the University of Saskatchewan, I agree that the Libraries of this University may make it freely available for inspection. I further agree that permission for copying of this thesis in any manner, in whole or in part, for scholarly purposes may be granted by the professor or professors who supervised my thesis work or, in their absence, by the Head of the Department or the Dean of the College in which my thesis work was done. It is understood that any copying or publication or use of this thesis or parts thereof for financial gain shall not be allowed without my written permission. It is also understood that due recognition shall be given to me and to the University of Saskatchewan in any scholarly use which may be made of any material in my thesis.

Requests for permission to copy or to make other use of material in this thesis in whole or part should be addressed to:

Head of the Department of Microbiology and Immunology
University of Saskatchewan
Health Science Building
107 Wiggins Road
Saskatoon, Saskatchewan, Canada S7N 5E5

ABSTRACT

APOBEC3G (Apo3G) is a host cell restriction factor of viruses that produce a single-stranded (ss) DNA replication intermediate (Sheehy et al., 2002; Suspene et al., 2004). Apo3G is studied primarily for its ability to restrict propagation of the retrovirus, HIV. In cell culture, Apo3G can only inhibit HIV if it lacks its virion infectivity factor (Vif). The host-pathogen interface between Apo3G and HIV has become a new target of study for the development of novel HIV therapeutics (Prochnow et al., 2009; Sheehy et al., 2003). Apo3G induces mutagenesis of the HIV proviral DNA (Mangeat et al., 2003; Zhang et al., 2003). Apo3G has the ability to induce transition mutations, i.e. cytosine to thymine, through deamination of cytosine to form uracil. Deamination activity induces numerous mutations that causes gene inactivation of the HIV provirus thus restricting the HIV lifecycle. Apo3G attenuates HIV virion infectivity in the absence of the virion infectivity factor (Vif) by inducing genome mutations through deamination of cytosine to uracil in HIV minus strand DNA. Independent from deaminase activity, Apo3G may also interfere with HIV reverse transcription by preventing full length cDNA from forming (Iwatani et al., 2007), nucleocapsid (NC) mediated strand annealing (Guo et al., 2007; Guo et al., 2009; Li et al., 2007), and RNaseH activity of the reverse transcriptase (Li et al., 2007). Whether Apo3G is able to restrict HIV by a deamination-independent mode remains controversial. In particular, the existence of the deamination independent mode was challenged since the Apo3G deamination null mutant E259Q was shown to have limited or no ability to inhibit HIV-1 replication (Schumacher et al., 2008). This research assesses the ability of Apo3G to inhibit reverse transcription of HIV genomic RNA. It is hypothesised that based on the ability of Apo3G to bind and oligomerize on single stranded nucleic acids (Chelico et al., 2008), and its high affinity for RNA (Chelico et al., 2010), that Apo3G can inhibit RT mediated primer extension as well as nucleocapsid mediated strand annealing. Additionally, it is hypothesized that Apo3G cannot inhibit RT RNAseH activity, as Apo3G has been shown to have a low affinity for DNA/RNA hybrids (Iwatani et al., 2006). We will test these hypotheses by using *in vitro* assays that mimic *in vivo* reverse transcription events.

Here we have shown that Apo3G is able to decrease the efficiency with which HIV-1 reverse transcriptase synthesizes DNA from an RNA primer annealed to an RNA template. Apo3G had a minimal affect on primer initiation and primarily inhibits primer elongation. Using

the monomeric mutant, F126A/W127A, we show that the deamination independent mode of inhibiting reverse transcriptase is impaired without oligomerization on template RNA. We also provide evidence that the Apo3G mutant E259Q should not be considered a deamination null proxy for native Apo3G since it exhibits decrease in RNA binding affinity compared to the native form. We did not find that Apo3G inhibited HIV NC-mediated strand annealing activity or RNaseH activity of HIV-1 reverse transcriptase. The data suggest a two-tiered mechanism for inhibition of reverse transcriptase-mediated DNA synthesis that is dependent upon 1) the ability of Apo3G to oligomerize on RNA substrates and 2) bind RNA with high affinity. Ascribing a mechanism to the deamination independent mode of HIV-1 restriction by Apo3G suggests that the enzyme may use this mechanism *in vivo* to delay completion of proviral DNA synthesis which, may negatively impact the HIV-1 lifecycle.

ACKNOWLEDGEMENTS

I first wish to thank Dr. Linda Chelico for accepting me as a graduate student in her lab. In her lab I was given all of the knowledge, advice and support that I needed to successfully complete my M.Sc. degree. Through lab meetings and informal discussions I was given the opportunity to learn a vast amount of knowledge within the realm of science. I am forever grateful for the opportunity to pursue a graduate degree in her lab.

I appreciate all of the guidance and advice that was provided to me by my advisory committee members. Dr. Sidney Hayes, Dr. Peter Howard and Dr. Joyce Wilson were an invaluable resource while I was in graduate studies. I would also like to thank Dr. Yuliang Wu for being my external examiner.

My wife Jennifer and I endured the hardship of living apart for several years while I completed my M.Sc. degree. I sincerely appreciate her undying support, understanding and patience while we lived apart during this time. Whenever I faced a challenge you were always just a phone call away.

The lab that I worked in during graduate studies was a fun and welcoming environment. This was made possible by the other graduate students in the lab. I would like to extend my many thanks to Robin Love and Anjuman Ara who made my graduate student experience enjoyable.

I would like to thank Dr. Brian Bandy (College of Pharmacy) for the use of his QM-4 spectrofluorometer. Additionally I would like to thank Dr. Nick Ovsenek for the use of his gel dryer. I would also like to thank The Saskatoon Cancer Centre and Dr. Vikram Misra (Veterinary Microbiology) for the use of their Bio-Rad FX Scanner and GE Healthcare Typhoon Scanner, respectively.

I am very grateful for the Establishment Grant funding that the Saskatchewan Health Research Foundation (SHRF) provided for my research. Having this funding made it possible for me to pursue graduate studies.

I wish to thank everyone in the department of Microbiology and Immunology for truly making me feel welcome to the department and for all of the support that they provided. I truly enjoyed working with everyone in the department.

I would like to thank my friends and family for being supportive while I pursued my dream of completing a M.Sc. degree. Their support helped me through many of the challenges that I faced while in graduate studies. Thanks for always being there.

TABLE OF CONTENTS

LIST OF TABLES

LIST OF FIGURES

LIST OF ABBREVIATIONS

AID	Activation Induced Deaminase
A	Adenine
K_d	Apparent dissociation constant
Apo3G	APOBEC3G
CD	Cytosine deaminase domain
C	Cytosine
dNTPs	Deoxynucleotide triphosphates
F/W	F126A/W127A
F	Fluorescein
F-Apo3G	Fluorescein labeled Apo3G
G	Guanine
HERVs	Human endogenous retroelements
kDa	Kilodalton
nM	Nanomolar
CD1	Cytosine deaminase domain 1
CD2	Cytosine deaminase domain 2
NC	Nucleocapsid
nt	Nucleotides
PAGE	Polyacrylamide Gel Electrophoresis
PPT	Polypurine tract
PNK	Polynucleotide kinase
PBS	Primer binding site
RT	Reverse transcriptase
ssDNA	Single-stranded DNA
TCR	T cell receptor
µM	Micromolar

U	Uracil
Vif	Virion infectivity factor

CHAPTER 1.0
INTRODUCTION

1.1 General overview of APOBEC and the HIV-APOBEC3 host-pathogen interface

APOBEC3G is a member of a larger family of genes in the Apolipoprotein B editing enzyme, catalytic polypeptide (APOBEC or Apo) family that catalyze the deamination of cytosine to uracil in either DNA or RNA (Sawyer et al., 2004). The members of this family are Activation Induced Deaminase (AID), Apo1, Apo2, Apo3A-H and Apo4 (Chiu and Greene, 2008). Two notable members of this family, apart from Apo3G, are Apo1 and AID. Apo1 edits the mRNA of apolipoprotein B which results is a truncated form of the apolipoprotein B lipid-transport protein, therefore modifying levels of low density lipoprotein production (Sawyer et al., 2004). AID is an important player in antibody maturation in B-lymphocytes , and it is involved in generating antibody diversity and antibody class-switching (Sawyer et al., 2004). The original function of the Apo3 subfamily of enzymes is believed to be inhibition of endogenous retroelements, such as retrotransposons Alu, LINE-1 or human endogenous retroelements (HERVs) (Chiu et al., 2006). Since retrotransposons are believed to be the origin of present day retroviruses and still display similar genetic replication features it is logical that Apo3 enzymes can act as potent inhibitors of both retrotransposons and retroviruses (Chiu et al., 2006). That cytosine deaminases benefit humans, demonstrates that there is reward in their mutagenic functions, when tightly controlled, that outweighs the risk of possible aberrant mutagenesis in the cell.

Apo3G, the first Apo3 enzyme discovered, was shown to potently restrict the infectivity of HIV virions in the absence of the HIV virion infectivity factor (Vif) (Sheehy et al., 2002). Virions that do not contain Vif are rendered noninfectious in the presence of Apo3G. Vif blocks the antiviral activity of Apo3G by interfering with Apo3G mRNA translation (Stopak et al., 2003), blocking virion encapsidation of Apo3G (Kao et al., 2003), blocking deamination activity of Apo3G (Santa-Marta et al., 2005), and by increasing Apo3G protein degradation in conjunction with the 26S proteasome (Sheehy et al., 2002; Stopak et al., 2003), therefore depleting Apo3G levels and creating a permissive cell phenotype. Vif-mediated protein degradation of Apo3G is considered the most potent form inhibiting Apo3G antiviral activity. Vif mimics an E3 ubiquitin ligase protein resulting in ubiquitination and degradation of Apo3G-Vif-E3 complexes (Yu et al., 2003). Vif likely evolved in HIV as a means of host immune system evasion. When Vif is absent, Apo3G renders HIV progeny virions noninfectious by deaminating cytosines to uracils in HIV cDNA or possibly by blocking synthesis of the proviral DNA. An overview of this host-pathogen interface is shown in Figure 1.1.

1.2 HIV Life-cycle/Replication

1.2.1 Viral Attachment and Entry

HIV utilizes host cellular receptors for attachment and entry. The cellular receptors that are primarily used are CD4, and either CCR5 or CXCR4 (Friedrich et al., 2011). CD4, a glycoprotein from the immunoglobulin superfamily, is expressed on helper and T regulatory cells, monocytes, macrophages, and dendritic cells and is a component of the T cell receptor (TCR) complex. Normally, CD4 binds to Class II MHC molecules during antigen presentation to T cells and TCR activation (Friedrich et al., 2011). The HIV surface glycoprotein, gp120, hijacks the CD4 molecule by binding to it upon attachment. Once gp120 is bound to CD4, conformational changes allow a second surface protein, gp41, to insert its fusion peptide into the host cell membrane. This ultimately facilitates viral fusion and host cell entry (Gorry and Ancuta, 2011).

1.2.2 Proviral DNA synthesis

Following viral attachment and entry, the positive (+) single stranded RNA genome of HIV must be converted into a double stranded DNA provirus before being integrated into the host genome. This occurs within the capsid. The HIV enzymes required for reverse transcription of genomic RNA to dsDNA the provirus are nucleocapsid (NC) and reverse transcriptase (RT). RT, which functions as a heterodimer (66 and 51 kDa subunits), is a DNA polymerase that synthesizes the first (-) and second (+) DNA strands, and also has an RNAseH domain that degrades the RNA strand within DNA/RNA hybrids (Coffin, 1997). During synthesis of the second strand of DNA, degraded RNA either spontaneously dissociates from the nascent DNA or is easily displaced by RT. The NC protein has sequence-nonspecific nucleic acid destabilization and strand annealing activity, collectively called chaperone activity, (Bampi et al., 2004; Rein et al., 1998) that are essential for removing RNA secondary structure and chaperoning priming events that enable RT to complete its role (Figure 1.2). First, NC unfolds and anneals the host $tRNA^{Lys,3}$ primer to the genomic RNA at a region near the 5'-end of the genomic RNA called the Primer Binding Site (PBS) to initiate synthesis of the minus strand DNA primer (strong stop DNA) (Figure 1.2 *Step 1 and 2*). The host $tRNA^{Lys,3}$ is specifically incorporated into the budding virion through an interaction with RT (Barat et al., 1989). Later, NC transfers the DNA/ $tRNA^{Lys,3}$ to 3'-end of the genomic RNA to prime (-)DNA synthesis (Bampi et al.,

2004) (Figure 1.2 *Step 3 and 4*). Second, NC transfers the (+) strand DNA, extended from the RNAseH-resistant polypurine tract (PPT) primers, to the 3'- end of the (-)DNA for second strand synthesis (Figure 1.2 *Step 5and 6*). NC also facilitates RT processivity (Grohmann et al., 2008).

Following viral entry into the host cell, RT gains access to the host cell pool of deoxynucleotide triphosphates (dNTPs). RT then recognizes the primer/template junction and begins incorporating dNTPs to synthesize (-) strand DNA (Coffin, 1997). During first strand synthesis, after the RNA is degraded, Apo3G is able to deaminate cytosines to uracils on the minus strand DNA. After completion of synthesis of the first DNA strand, the RT uses two RNAseH degradation resistant Polypurine Tracts (PPT) in the genomic RNA to prime second strand synthesis. Synthesis of the second strand of DNA blocks any further Apo3G deaminations, but it also seals in the mutations induced by Apo3G. RT is highly error prone (Coffin, 1997), which is an advantage for HIV as the RT induced mutations help HIV to rapidly evolve and adapt. However, the mutations induced by Apo3G overcome the evolutionary flexibility in the HIV genome and cause gene inactivation (Pillai et al., 2008).

1.2.3 Integration, Assembly and Exit

Once reverse transcription is completed, the HIV proviral DNA is integrated into the host cell genomic DNA. Recent models favor the uncoating of the viral capsid to allow nuclear entry (Arhel, 2010). HIV uses virus encoded integrase to insert proviral DNA into the host genome (Coffin, 1997). Once integrated, the provirus is transcribed using the host RNA polymerase. Initial transcription events produce RNA that is translated into proteins. Late RNA synthesis produces nascent genomic RNA which is incorporated into assembling virions (Coffin, 1997). To restrict HIV, Apo3G must be incorporated into assembling virus particles. Incorporation involves the interaction of Apo3G with the NC region of the Gag polyprotein and/or RNA (Strebel and Khan, 2008). It is thought that Apo3G can interact with either 7SL RNA or viral RNA in order to be incorporated into the nucleoprotein complex of the newly budding virions (Strebel and Khan, 2008). Since Apo3G is compartmentalized in cellular RNA processing bodies (Gallois-Montbrun et al., 2006), it must bind to RNA that will be encapsidated into the virion in order to escape to another cellular localization (Soros et al., 2007). Only 7 ± 4 Apo3G molecules are encapsidated and are sufficient to hinder HIV replication upon a subsequent round of infection (Xu et al., 2007).

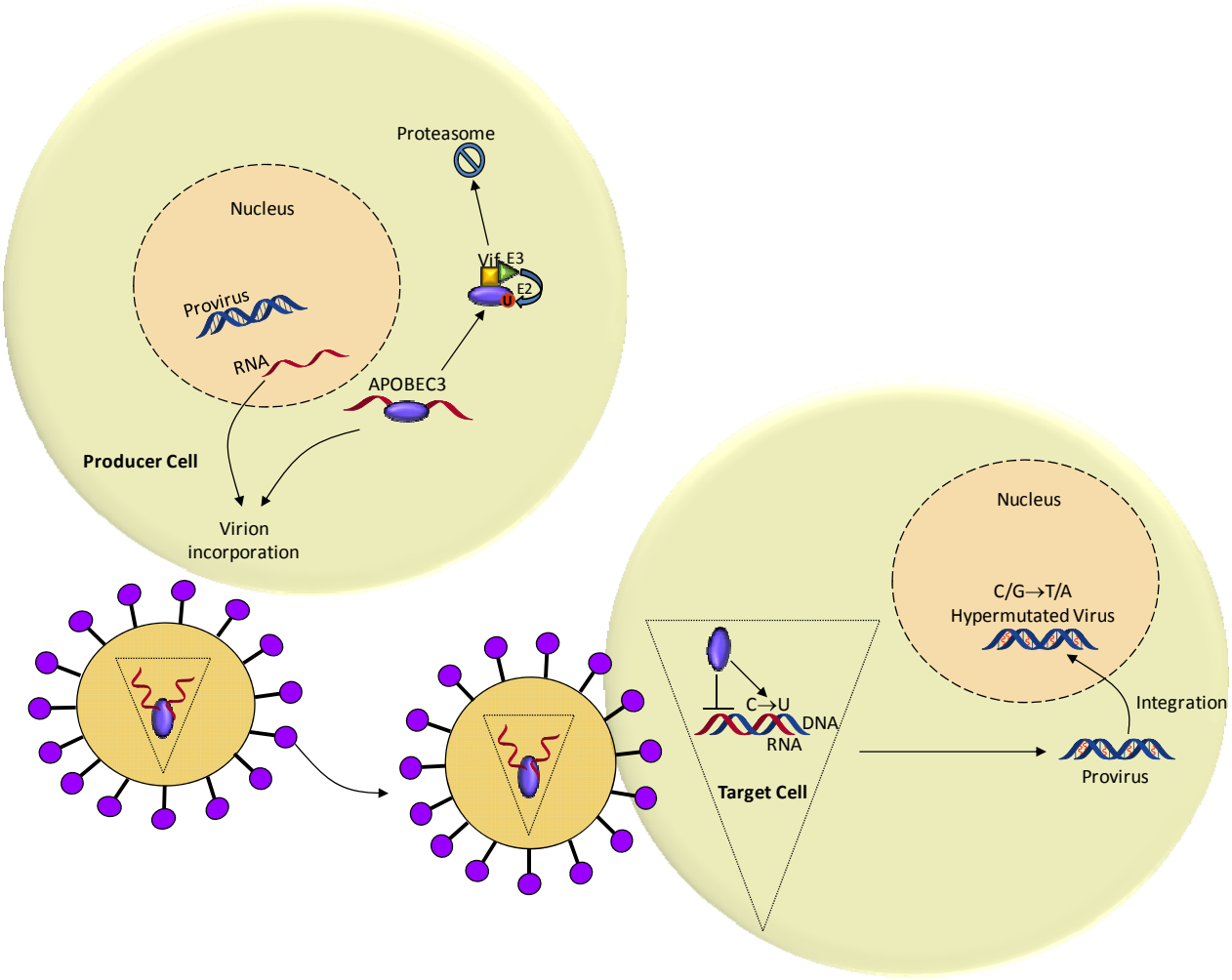

Figure 1.1 **Inhibition of HIV by APOBEC3G that escapes Vif mediated degradation.** HIV Vif interacts with a cellular ubiquitin ligase complex to become the substrate recognition subunit of an E3 ubiquitin ligase. The Vif-E3 complex recruits an E2 enzyme that transfers ubiquitin molecules to Apo3G, thereby signaling it for degradation through the proteasome pathway. Apo3G that escapes degradation either fortuitously, or in the presence of a Vif-defective HIV strain, can enter an assembling virus particle through interactions with RNA (host 7SL RNA or HIV genomic RNA) and the NC portion of Gag. Then, Apo3G travels with the HIV particle to the next target cell, akin to a 'Trojan Horse', where it awaits for reverse transcription of the HIV genomic RNA to (-) DNA. Apo3G, a single-stranded DNA deaminase is able to deaminate cytosine (C) to uracil (U) in (-) DNA, and causes the RT to introduce guanine (G) to adenine (A) mutations upon using uracil-containing (-) DNA as a template to synthesize (+) DNA. This creates a hypermutated and likely inactivated virus. Apo3G may also physically inhibit the accumulation of reverse transcripts in a manner that is deamination independent.

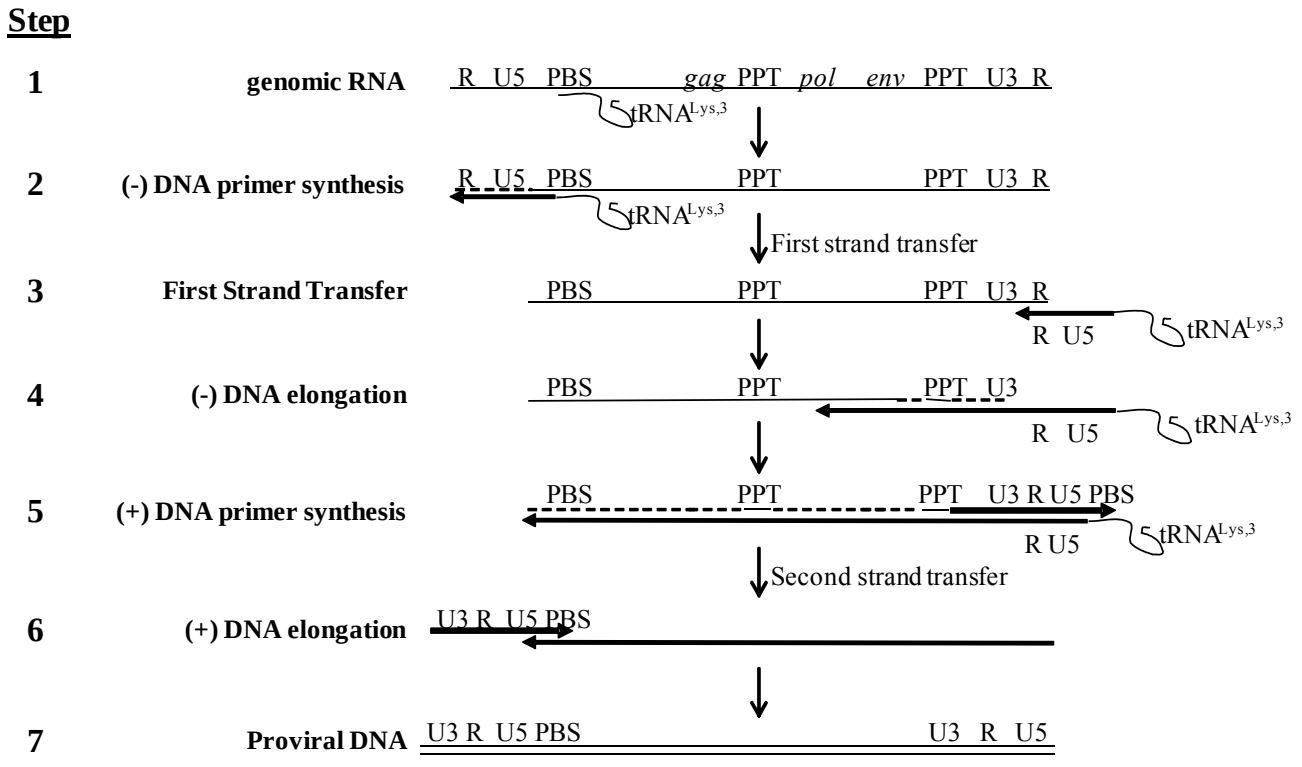

Figure 1.2 **Schematic of reverse transcription and replication of the HIV RNA genome into the proviral DNA.** The genomic RNA (*black line*) is primed for replication using a host $tRNA^{Lys,3}$ primer (*Step 1)*. The NC protein facilitates the transfer of primers to initiate first strand ((-)DNA) and second strand ((+)DNA) synthesis (*Steps 2 and 5*). The RT synthesizes the DNA (*bold line*) and degrades the RNA (*hatched line*) with its RNAseH domain (*Steps 4 and 6*). In the time between (-)DNA synthesis and (+)DNA synthesis, single-stranded regions of the (-)DNA become substrates for Apo3G-catalyzed deaminations. Abbreviations are: R, repeated sequence; U5, unique 5'-region; PBS, primer binding site; PPT, polypurine tract; U3, unique 3'-region.

1.3 Biochemistry of APOBEC3G

1.3.1 APOBEC3G Deamination activity *in vitro*

Apo3G has two cytosine deaminase domains (CD) in contrast to APOBEC1 and AID which have only one domain (Chiu and Greene, 2008). The domains are known as CD1 and CD2 and are located in the N- and C- termini of the enzyme, respectively. However, in Apo3G, only the CD2 is

catalytically active. The CD1 is able to bind nucleic acids and is necessary for incorporation of Apo3G into HIV virions (Navarro et al 2005). The CDs of all APOBEC family members can be characterized as having a consensus zinc-binding deaminase motif His-X-Glu-X_{23-28}-Pro-Cys-X_{2-4}-Cys, where X symbolizes any amino acid (Harris and Liddament, 2004). The cytosine deaminases harbor similar core structural features, including a typical core β-sheet consisting of five β-strands and an active site containing a zinc atom coordinated by three residues (two Cys and a His/Cys) from the second and third helices (Bransteitter et al., 2009). This is a canonical type of zinc coordination with a centrally located Zn atom that can interact with a water molecule and become activated. The water molecule serves as a hydrogen donor during the deamination process. The conserved glutamate residue, E259 in Apo3G, facilitates catalysis by it functioning as a proton shuffler for the hydrolytic reaction (Bransteitter et al., 2009). The glutamate residue is likely responsible for the amine group removal from cytosine, which forms uracil (Harris and Liddament, 2004), as shown in Figure 1.3A. The deamination reaction of Apo3G shows marked specificity for 5'CCC repeats (Chelico et al., 2006). Apo3G deaminates cytosine processively, meaning that it has the ability to deaminate multiple cytosine residues on a single DNA target before dissociation (Chelico et al., 2006).

1.3.2 APOBEC3G oligomerization

Apo3G has been shown to form oligomers and exists as monomers, dimers, tetramers and even higher order structures (Chelico et al., 2010; Chelico et al., 2008). In solution, Apo3G is a monomer or dimer. Upon binding ssDNA or RNA, Apo3G oligomerizes into dimers, tetramers and higher order structures (Chelico et al., 2010; Chelico et al., 2008). The F126A/W127A (F/W) mutant, which has been shown to exist as a monomer in solution and when bound to DNA or RNA, demonstrates that Apo3G dimerization is specific to a region in the N-terminus and tetramer formation through the C-terminus is hierarchically dependent on dimerization (Chelico et al., 2010; Huthoff et al., 2009).

1.4 Clinical studies of APOBEC3G inhibition of HIV

Apo3G is the model deaminase from the Apo3 family and appears to be the most effective restrictor of HIV replication as measured by cell-based assays (Bishop et al., 2004; Han et al., 2004; Zennou and Bieniasz, 2006) and suggested by mRNA expression (Koning et al., 2009; Refsland et al., 2010) and clinical studies (Biasin et al., 2007; Knopp et al., 2003; Patel et al., 2002; Ulenga et al.,

2008; Vazquez-Perez et al., 2009; Xu et al., 2003). Clinical subjects found to have an inherent ability to express a high level of Apo3G are less likely to become infected with HIV or progress from HIV to AIDS (Biasin et al., 2007; Knopp et al., 2003; Koning et al., 2009; Patel et al., 2002; Refsland et al., 2010; Ulenga et al., 2008; Vazquez-Perez et al., 2009; Xu et al., 2003). Evidence of deaminations in HIV genomes recovered from patients carry C/G→T/A mutations in a sequence context that indicates deaminations by Apo3G occur most frequently (Knopp et al., 2003; Patel et al., 2002; Vazquez-Perez et al., 2009).

Further evidence of the clinical relevance of Apo3G is from the clinical Apo3G mutant, H186R. Accelerated AIDS progression is associated with the clinical Apo3G mutant H186R. This single nucleotide polymorphic variant has been shown to be prevalent among African Americans and rare in European Americans or Europeans (An et al., 2004). When present in HIV positive African Americans, the H186R mutation is associated with accelerated AIDS progression. The H186R mutant has been found to have an altered processive mechanism compared to native Apo3G that leads to fewer deamination-induced mutations in a reconstituted HIV replication system (Feng and Chelico 2011). The biochemical difference may contribute to the decreased effectiveness seen in clinical studies.

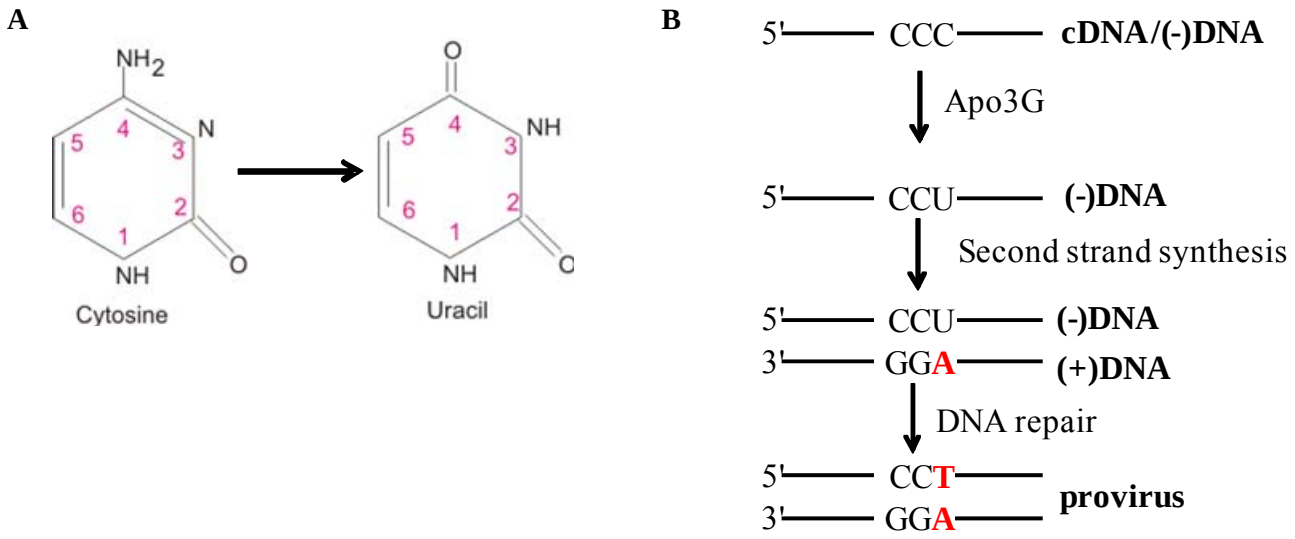

Figure 1.3 **Deamination of cytosine to uracil in DNA is mutagenic.** (A) Apo3G catalyzes the deamination of cytosine (*position 4*), to form uracil. Uracil is mutagenic in DNA because when polymerases encounter uracil in the template during DNA synthesis, the original C/G basepair is converted to a T/A basepair. (B) Illustration of how cytosine deamination can lead to a mutation. Apo3G can deaminate cytosines on the first strand of DNA synthesized ((-)DNA) from the RNA genome of HIV. Apo3G prefers to deaminate the third C in the motif, 5'CCC. Upon synthesis of the second strand of DNA ((+) DNA), the reverse transcriptase of HIV will "read" the uracil as a thymine and insert an adenine while the original genome sequence had a guanine at this position. Apo3G catalyzes deaminations at numerous positions on the HIV (-) DNA. Multiple A/T base pair substitutions result in production of defective viral proteins and loss of infectivity.

1.5 Modes of HIV restriction by APOBEC3G

There are two possible modes by which Apo3G functions to thwart HIV, one mode being deamination dependent and the other mode being deamination independent. Deamination and its effects on HIV have been unequivocally demonstrated (Mangeat et al., 2003; Zhang et al., 2003). However, whether a deamination independent mode exists remains controversial. Since the deamination independent mode would occur first, to inhibit minus strand synthesis, then the deamination based mode could be considered only a back-up mechanism for Apo3G. This hypothesis has merit since the original function of inhibiting retrotransposons by Apo3G occurred solely by binding transposon RNA and shuttling it to RNA degradation bodies, a deamination independent

mechanism (Chiu et al., 2006).

1.5.1 Deamination dependent mode of APOBEC3G inhibition of HIV

The result of the deamination dependent mode is the deamination of cytosine to uracil in the first strand of DNA synthesized from the HIV RNA genome. Since Apo3G is a single-stranded DNA deaminase, the deamination activity is limited to the first strand of DNA only (Figure 1.2). The minus strand then serves as a template for plus strand synthesis and the dU residues are templates for the incorporation of dA (Figure 1.3B). The result is a dG-to-dA hypermutated virus with an altered viral open-reading frame having nonsense and missense mutations (Chiu and Greene, 2009). In addition to this, accumulating dUs in the minus strand DNA may lead to a decrease in plus strand synthesis due to aberrant initiation (Chiu and Greene, 2009).

1.5.2 Deamination independent mode of APOBEC3G inhibition of HIV

The literature concerning the deamination independent mode of Apo3G is filled with controversial reports. The deamination independent mode has been shown to decrease the accumulation of early and late reverse transcripts by up to 50-90% (Bishop et al., 2006; Guo et al., 2006; Iwatani et al., 2007; Li et al., 2007; Mangeat et al., 2003; Newman et al., 2005). However, others have reported that Apo3G does not have a deamination independent mode and claim that deamination is the only mode that Apo3G utilizes to restrict HIV (Mbisa et al., 2007; Miyagi et al., 2007; Schumacher et al., 2008).

In this M.Sc. research project we used a new research approach, a series of stepwise focused biochemical experiments, to reconcile the literature in the field. For those who do subscribe to a deamination independent mode there are two competing theories that are the most prevalent; that Apo3G inhibits RT polymerization and possibly RNAseH activity (Iwatani et al., 2007; Li et al., 2007) or that Apo3G inhibits NC mediated RNA annealing (Guo et al., 2006).

Apo3G inhibition of RT polymerization was concluded to be evident since it reduces the accumulation of reverse transcripts *in vivo* (Mangeat et al., 2003). One theory is that the ability of Apo3G to bind nucleic acids is central to its deamination independent mechanism. It has been hypothesized that the N-terminal domain (CD1) binds to viral RNA/DNA and decreases the polymerization efficiency of RT (Iwatani et al., 2007). The steady state dissociation constant (K_d) of

Apo3G for bacteriophage lambda DNA is 8- fold less than that of RT so Iwatani *et al* concluded that Apo3G could successfully out compete RT for DNA/RNA substrates (Iwatani et al., 2007). This characteristic is likely due to the ability of Apo3G to oligomerize on nucleic acids into dimers, tetramers, and other higher order forms (Chelico et al., 2008). It is also hypothesized that Apo3G can interact directly with RT (Douaisi et al., 2004). Although one study found that there was no direct interaction between Apo3G and RT (Iwatani et al., 2007), another study, based on qualitative data from immunoprecipitation assays, found that that Apo3G and RT likely interact (Douaisi et al., 2004). The hypothesis of Douaisi et al. is that Apo3G may act by binding to RT and reducing its activity.

The doubts in the existence of a deamination independent mode came from two lines of evidence. First, some research groups found that the decrease in the accumulation of HIV reverse transcripts only occurred at a high transfection level of exogenous Apo3G into 293T cells (Miyagi et al., 2007; Schumacher et al., 2008). When transfection levels were decreased to mimic cellular levels of Apo3G the deamination independent mode of inhibition was not detected. Second, the catalytically inactive mutant of Apo3G, E259Q, has been used to test the deamination independent mode of inhibition as groups have seen a 40-100% decline in the inhibition of reverse transcripts, suggesting that deamination is necessary (Bishop et al., 2008; Mbisa et al., 2007; Miyagi et al., 2007; Schumacher et al., 2008). However in research that has used the E259Q mutant as a "control" for a deamination null form of Apo3G, it has never been established that despite lacking deamination activity, this mutant is a biochemically equivalent version of Apo3G. Mutating regions of an enzyme near the Zn coordination residues can cause structural changes since the Zn molecule is an important part of the internal scaffold of enzyme structure.

1.6 Hypothesis and Objectives

This research project will assess the ability of Apo3G to inhibit events necessary for reverse transcription of HIV genomic RNA. It is hypothesized that Apo3G can inhibit RT mediated primer extension and nucleocapsid (NC) strand annealing though the ability of Apo3G to bind and oligomerize on single stranded nucleic acids (Chelico et al., 2008). Unless we find that there is a strong protein-protein interaction between RT and Apo3G, it is hypothesized that Apo3G cannot inhibit RNAseH activity of RT because of a low affinity for binding DNA/RNA hybrids (Iwatani et al., 2006).

We are mindful that the research is *in vitro* and will be using levels of enzymes that mimic the concentrations encountered in a virion *in vivo* (Table 1.1). The concentrations of enzymes and RNA

were added at ratios that mimic the predicted concentration in a *ΔVif* HIV virion with a 60 nm radius (Briggs et al., 2004; Coffin, 1997; Xu et al., 2007; Zhu et al., 2003a).

This aim of this project is to assess the deamination independent mode that Apo3G potentially utilizes to restrict HIV through the following approaches:

(1) Testing to see if Apo3G can inhibit polymerization of a primer/template by RT or degradation of the genomic RNA by the RNAseH domain of RT after cDNA synthesis.

- Here we have used *in vitro* assays using radionucleotide labeled substrates to detect either polymerization efficiency or RNAseH degradation efficiency.

(2) Testing to see if Apo3G can interfere with the first strand primer ($tRNA^{Lys,3}$) annealing in the PBS of the HIV genome. This step is critical for minus strand DNA synthesis and is mediated by NC.

- Here we have used an established strand annealing assay used to study NC strand annealing activity.

(3) Establishing the mechanism of inhibition using experiments that will be designed based on results of objectives (1) and (2).

- Here we have used the technique of rotational anisotropy (fluorescence depolarization) to quantify protein-protein or protein-nucleic acid interactions.

Table 1.1 **Estimated concentration of reverse transcription components in an HIV-1 virion.**

	Number molecules per virion	Concentration (60 nm virion radius)	Molar ratio to genome	Reference
genomic RNA	2	3.7 μM	--	(Coffin, 1997)
nucleocapsid	1400-5000	6 ± 3 mM	1621 ×	(Briggs et al., 2004; Zhu et al., 2003b)
reverse transcriptase	100	180 μM	48 ×	(Coffin, 1997)
Vif	7-20	25 ± 12 μM	7 ×	(Camaur and Trono, 1996)
Apo3G (*Δvif* HIV-1)	3-11	13 ± 8 μM	4 ×	(Xu et al., 2007)

CHAPTER 2.0
METHODOLOGY

2.1 Site-directed mutagenesis and cloning

Primers are listed in Table 2.1 and were purchased from Integrated DNA Technologies. Site-directed mutagenesis to construct the Apo3G E259Q clone was conducted previously in our lab (unpublished data) using the QuikChange site-directed mutagenesis protocol with the pAcG2T-Apo3G vector as the template (Chelico et al., 2006). Construction of native Apo3G, Apo3G F126A/W127A (F/W mutant), and NC have been described previously (Chelico et al., 2010; Feng and Chelico, 2011).

For the RNA template, a 104-nucleotide (nt) segment near the 5'-end of the HIV-1 genome (nt 571-674, Table 2.1) from the HIV-1 clone 93th253.3 (GenBank accession number U51189) encompassing the PBS and upstream region was PCR amplified and cloned into the BamHI and EcoRI sites of the pSP72 vector (Promega). The HIV-1 clone was obtained through the AIDS Research and Reference Reagent Program, Division of AIDS, NIAID, National Institutes of Health; p93TH253.3 was from Dr. Feng Gao and Dr. Beatrice Hahn (Gao et al., 1996).

2.2 Protein expression and purification

Recombinant baculoviruses expressing GST-NC and GST-Apo3G proteins (native and mutant) was constructed as described previously (Chelico et al., 2006; Feng and Chelico, 2011). *Sf*9 cells were infected with recombinant NC or Apo3G virus at a multiplicity of infection of 1 and harvested after 72 h. Cells were lysed and proteins purified, as described previously, to obtain NC or Apo3G protein cleaved from the GST tag (Chelico et al., 2010; Feng and Chelico, 2011). Cleaved protein fractions were stored at −70 °C. The NC and Apo3G forms are >95% pure. Proteins were previously purified in the lab except E259Q which was purified for this study. Purified HIV-1 RT p66/p51 (Le Grice and GrÜNinger-Leitch, 1990) was generously provided by Dr. Stuart F. J. Le Grice (NCI, National Institutes of Health).

2.2.1 Protein Purity

Two micrograms of purified native, F/W, E259Q and H186R Apo3G were resolved by 12% SDS-Polyacrylamide Gel Electrophoresis (PAGE). Before loading, the proteins were denatured by addition to 1x SDS sample buffer (50 mM Tris pH 6.8, 2% SDS, 10% glycerol, 1% β-mercaptoethanol, 12.5 mM EDTA, 0.02% bromophenol blue) and heating at 65ºC for one minute. The SDS-PAGE gel

was resolved at 150 Volts until the bromophenol blue reached the bottom of the gel. The gel was then stained with coommassie (0.1% coommassie blue R-250, 45% methanol, and 10% glacial acetic acid). The gel was then destained in 10% glacial acetic acid and 10% Methanol and visualized with a Bio-Rad Chemidoc (Figure 2.1).

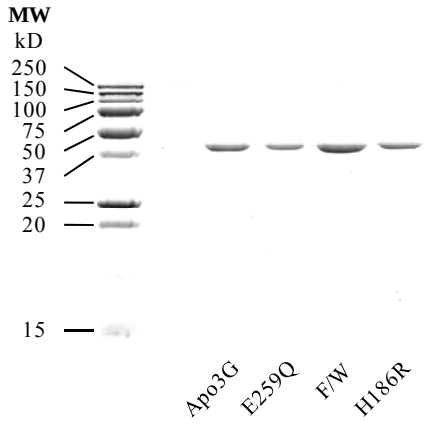

Figure 2.1 **Protein purity verification** Native, E259Q, F/W and H186R Apo3G were resolved on a 12 % SDS-PAGE gel and stained with coommassie. Native and mutant Apo3G (46.4 kDa) resolve as a ~ 40 kDa protein. This gel verifies the enzymes are >95% pure.

2.3 *In vitro* RNA production

The pSP72-RNA template vector described in Section 2.1 was purified from DH5α *Escherichia coli* and linearized with EcoRI to be used as a substrate for T7 RNA polymerase-mediated transcription, as per manufacturer's instructions for RNA (Promega) or fluorescein (F) labeled (F-UTP) RNA (Roche).

2.4 Radiolabeling of oligonucleotides

2.4.1 5'-end labeling of synthetic RNA

One micromolar of the RNA Primer (Table 2.1) was labeled in a 10 µL reaction consisting of 1 unit of Polynucleotide Kinase (PNK) (New England Biolabs), 1X PNK buffer, 700 nM of γ-^{32}P ATP (6000 Ci/mmol, Perkin –Elmer), and 4.75 µL of ddH_2O. The reaction was heated at 37 ºC for 45 min and then the PNK was inactivated by heating at 95 ºC for 10 min.

2.4.2 5'-end labeling of *in vitro* transcribed RNA

The template RNA was produced by *in vitro* T7 polymerase mediated transcription, as described in Section 2.3. Radiolabeling was accomplished by first dephosphorylating the template RNA with 2 units of Antarctic Phosphatase (New England Biolabs) according to the manufacturer's instructions with provided buffer in a 10 µL reaction, which was scaled up accordingly, at 37 ^{o}C for 60 min with subsequent heat inactivation at 65 ^{o}C for 5 min. The 5'-end dephosphorylated RNA was then 5'-end labeled using γ-^{32}P-ATP using a 70 % labeling efficiency (6000 Ci/mmol, Perkin –Elmer) with 2 units of Polynucleotide Kinase (New England Biolabs) in a 10 µL reaction, which was scaled up accordingly, at 37 ^{o}C for 45 min with subsequent heat inactivation at 95 ^{o}C for 10 min.

2.4.3 Internal labeling of *in vitro* transcribed RNA

Internally α-^{32}P CTP labeled RNA template was synthesized using a Riboprobe® *in vitro* Transcription kit (Promega). The 20 µL labeling reaction consisted of 4µL of Transcription Buffer (Promega), 2µL of 100 nM DTT, 20u of Recombinant RNasin® Ribonuclease Inhibitor (New England Biolabs), 4µL of a solution containing 2.5 mM rATP, rGTP, and rUTP, 2.4 µL of 100 µM rCTP, 1 µL of 1.0 mg/ml linearized template DNA, 50 µCi α-^{32}P CTP in 5 µL and 1µL of T7 RNA Polymerase. The reaction was incubated for 1 hr at 37ºC. Following this, 1uL of DNAseI was added to the reaction and was incubated for 15 minutes at 37ºC. The internally labeled template RNA was then purified by extraction with low pH Phenol:Chloroform (Ambion). The recovered aqueous phase was passed through a P-6 Biospin column (Bio-Rad) to remove unincorporated nucleotides.

2.5 Nucleocapsid-mediated strand annealing assay

The annealing assay reactions contained 5' end labeled template RNA (Section 2.4.2, 20 nM), Human tRNA^{Lys,3} (40 nM, BioS&T Montreal, Quebec), annealing assay buffer (20 mM Tris pH 7.5, 30 mM NaCl, 0.1 mM $MgCl_2$, 10 µM $ZnCl_2$ and 5 mM DTT), Recombinant RNasin® Ribonuclease Inhibitor (1unit, New England Biolabs), and NC (50-1700 nM). Native, E259Q, F/W mutant and H186R Apo3G were added at either 80 nM or 640 nM concentrations. Samples of 2.5 µL were taken at 5, 10 and 30 min and stopped by adding the sample to a solution which contained 0.5 mg/ml Proteinase K (New England Biolabs) in annealing assay buffer and incubated at 20^{o}C for 20 min.

Afterwards, loading dye was added to a concentration of 1x (50 mM Tris, pH 7.5, 4% glycerol, 0.01% w/v xylene cyanol, and 0.01% w/v bromophenol blue). Two and a half microlitres of sample were resolved on an 8% non-denaturing polyacrylamide gel. The gels were then dried for 2 hours and the bands were visualized by phosphorimaging with a Typhoon phosphorimager (GE Healthcare).

2.6 Primer extension assay

Primer extension assays were employed to measure RT elongation activity with and without Native Apo3G and mutant enzymes. The template RNA was heat annealed to a 5'-^{32}P-labelled synthetic RNA primer (Section 2.4.1, Table 2.1). The primer/template (20 nM) was then used in reactions containing RT buffer (50mM Tris, pH 7.5, 40 mM KCl, 10 mM $MgCl_2$, 1 mM DTT), 500 μM dNTPs, 960 nM RT with or without 350 nM NC, and Apo3G (native, F/W mutant, E259Q, or H186R) at either 80 or 640 nM. Reactions were preincubated at 37 °C for 1 min before the addition of dNTPs which were used to start the RT elongation reaction. The enzymes were added at specific ratios to the primer/template to mimic the predicted concentrations in an HIV virion with a 60 nm radius (Briggs et al., 2004; Coffin, 1997; Xu et al., 2007; Zhu et al., 2003a), excluding the reaction with 640 nM of Apo3G. Reactions were stopped by adding a 4-fold excess of 20 mM EDTA and 95% formamide. Primer extension was visualized by resolving samples on a 16% denaturing urea-polyacrylamide gel. Gel band intensities were measured by phosphorimaging with a Bio-Rad FX scanner or Typhoon imager (GE Healthcare) and analyzed with ImageQuant software (GE Healthcare).

2.7 Rotational anisotropy

2.7.1 Protein-RNA steady state rotational anisotropy assays

Rotational anisotropy was measured with a QuantaMaster QM-4 fluorometer (Photon Technology International). Fluorescein labeled samples were excited with vertically polarized light at 494 nm, and both vertical and horizontal emissions were monitored at 520 nm (3.5-nm band pass).

2.7.1.1 Reverse transcriptase and APOBEC3G with RNA

To measure the affinity of RT and Apo3G (Native and mutant enzymes) for the primer/template RNA, Protein-RNA steady state rotational anisotropy assays were utilized. A 5'-end fluorescein

labeled RNA primer (Integrated DNA Technologies) (Table 2.1) was heat annealed to the template RNA to form the primer/template binding substrate at a ratio of 1:1.5. The reactions (80 μL) were incubated at 37 °C and contained RT buffer and primer/template (30 nM). Increasing concentrations (0-2100 nM) of either RT, native Apo3G, F/W mutant or E259Q were then added to the primer/template containing RT buffer.

2.7.1.2 Nucleocapsid and APOBEC3G with RNA

To measure NC and Apo3G binding, a fluorescein labeled template RNA (Section 2.3) was used as the binding substrate for experiments involving Apo3G and NC. The reactions (80 μL) were incubated at 37 °C and contained RT buffer, fluorescein labeled template RNA (50nM), and either increasing concentrations of Apo3G (0-2100 nM) with or without 500 nM or 850 nM NC prebound to the fluorescein labeled template RNA or increasing concentrations of NC (0-2100 nM) with or without 500 nM or 850 nM Apo3G prebound to the fluorescein labeled template RNA.

Rotational anisotropy was measured with a QuantaMaster QM-4 fluorometer (Photon Technology International). Samples were excited with vertically polarized light at 494 nm, and both vertical and horizontal emissions were monitored at 520 nm (3.5-nm band pass).

2.7.2 Protein-Protein steady state rotational anisotropy assays

To measure how Apo3G interacted with RT and the F/W mutant, Protein-Protein steady state rotational anisotropy assays were employed. Native Apo3G was labeled with flourescein (F) using the Fluorescein-EX Protein Labeling Kit (Molecular Probes). Fifty nanomolar of F-Apo3G was used in a reaction mixture (80 μL) containing RT buffer and a titration of RT, native Apo3G or F/W mutant (0-11 μM). Reactions were monitored at 37 °C. Rotational anisotropy was measured using a QuantaMaster QM-4 fluorometer (Photon Technology International) with a single emission channel. Samples were excited with vertically polarized light at 494 nm, and both vertical and horizontal emission were monitored at 520 nm (5 nm band pass).

2.8 Electrophoretic mobility shift assay

To assess the ability of Apo3G and mutant enzymes to compete with RT for binding the primer

template (Table 2.1), electrophoretic mobility shift assays were utilized. A 5'-end fluorescein labeled RNA primer (Integrated DNA Technologies) (Table 2.1) was heat annealed to the template RNA (Table 2.1) at a ratio of 1:1.5 to form a primer/template binding substrate. The reactions (10 μL) were incubated for 5 minutes at 25 °C and contained RT buffer, primer template (50 nM), and 4% glycerol, with or without prebound native Apo3G (480 nM). Increasing concentrations of RT (0-2480 nM) were added to the reaction. Band shifting, indicating RNA binding, was visualized by resolving samples on an 8% non-denaturing polyacrylamide gel. Gel bands were visualized by scanning with a Typhoon imager (GE Healthcare).

2.9 Pyrrolo-C fluorescence based assay

The detection of protein induced conformational changes in primer/template RNA that may be caused by Native Apo3G and the F/W and E259Q mutants was assessed by using Pyrrolo-C florescence assays. Pyrollo-dC is a fluorescent nucleotide analogue that can be used to monitor changes in the local structure of the ssDNA (Chelico et al., 2008). A 60 nt pyrrolo-C labeled RNA (100nM) (Table 2.1), purchased from Tri-Link Biotechnologies, was added to a reaction mixture (80 μL) containing 50 mM Tris, pH 7.5, 2.5 mM $MgCl_2$ and 1.2 μM of either native Apo3G, E259Q or F/W mutant. Reactions were incubated at 25 °C. Samples were excited at 345 nM (10 nm band pass) and the emissions were scanned (1 nm/second) with a range from 410-510 nM. The 450 nm emissions peak was used to calculate the relative fluorescence emissions of each enzyme with the RNA compared to RNA alone.

2.10 RNAseH assay

To determine the ability of Apo3G and mutant enzymes to inhibit RT mediated RNAse H activity, RNAseH assays were used. Internally α-^{32}P CTP radiolabelled RNA (20 nM, Section 2.4.2) was either annealed to a full length complementary DNA or an RNA primer (Table 2.1). The relevant substrate was then used in reactions containing RT buffer, 500 μM dNTPs, 960 nM RT, 350 nM NC, in the absence or presence of Apo3G (native, F/W mutant, E259Q, or H186R) at either 80 or 640 nM.

The enzymes were added at specific ratios to the primer/template to mimic the predicted concentrations in an HIV virion with a 60 nm radius (Briggs et al., 2004; Coffin, 1997; Xu et al., 2007; Zhu et al., 2003a), excluding the reaction with 640 nM of Apo3G. Reactions were stopped by adding a

4-fold excess of 20 mM EDTA and 95% formamide. RNA degradation was visualized by resolving samples on a 16% denaturing urea-polyacrylamide gel. Gel band intensities were measured by phosphorimaging with Typhoon imager (GE Healthcare) and analysis with ImageQuant software (GE Healthcare).

Table 2.1 **Primers and substrates.**

Name	Sequence
E259Q SDM Forward	CCT TGA AGG CCG CCA TGC ACA GCT GTG CTT CCT GGA CGT GAT TC
E259Q SDM Reverse	GAA TCA CGT CCA GGA AGC ACA GCT GTG CAT GGC GGC CTT CAA GG
Template RNA cloning primer (Forward)	GAA TTC CCC TAT TAA CTT TCG CTT TCA AG
Template RNA cloning primer (Reverse)	AGA TCT TGT TAG GAC TCT GGT AAC TAG AG
Template RNA	UGU UAG GAC UCU GGU AAC UAG AGA UCC CUC AGA UCA CUC UAG ACU GAG UAA AAA UCU CUA GCA GUG GCG CCC GAA CAG GGA CUU GAA AGC GAA AGU UAA UAG GG
Full Complement DNA	CCC TAT TAA CTT TCG CTT TCA AGT CCC TGT TCG GGC GCC ACT GCT AGA GAT TTT TAC TCA GTC TAG AGT GAT CTG AGG GAT CTC TAG TTA CCA GAG TCC TAA CA
RNA Primer	GUC CCU GUU CGG GCG CCA CUG CUA
Fluorescein labeled RNA primer	(FAM)GU CCU GUU CGG GCG CCA CUG CUA
Pyrrolo-C RNA	AUU AUU AUU AUU AUU AUU AUU CCC CC(P-C) AUU UAU UUA UUU A CCC CCC AUU UAU AUU AUU AU

Abbreviations: FAM is fluorescein, P-C is pyrrolo-C.

CHAPTER 3.0
RESULTS

3.1 The influence of APOBEC3G on Nucleocapsid-mediated $tRNA^{Lys,3}$ annealing

3.1.1 The effect of APOBEC3G on Nucleocapsid-mediated annealing of $tRNA^{Lys,3}$ to the primer binding site of HIV RNA

We hypothesized that since Apo3G can bind to RNA that it might inhibit the ability of NC to facilitate the annealing of $tRNA^{Lys,3}$ to the RNA. This assay was chosen as it models the initial step of HIV replication, the annealing of the host $tRNA^{Lys,3}$ to the HIV genomic PBS. The ^{32}P-labelled 104 nt single stranded template RNA containing the PBS region is incubated with a folded $tRNA^{Lys,3}$ and NC in the absence or presence of Apo3G. Annealing of the $tRNA^{Lys,3}$ to the template RNA is monitored by the formation of a higher molecular weight product on the gel. By itself the ^{32}P-labelled template RNA appears as a single band (Figure 3.1, *lane 1*). When $tRNA^{Lys,3}$ is heat annealed to the RNA the band shifts upwards due to an increase in mass (Figure 3.1, *lane 3*). When $tRNA^{Lys,3}$ is added without heat annealing to the RNA, no discernible band shifts are detected because the $tRNA^{Lys,3}$ requires unfolding by NC. When NC and the $tRNA^{Lys,3}$ are present with the template RNA, band shifts are detected as early as 5 min and increase in population after 10 and 30 minutes (Figure 3.1, *lanes 4,5 and 6, respectively*). This demonstrates that the *in vitro* assay can model NC-mediated strand annealing of $tRNA^{Lys,3}$ to the HIV PBS embedded within the RNA.

However, when Apo3G is added to the reaction at a ratio of 4 Apo3G: 1 template RNA, the ratio estimated to be present in virions (see Table 2.1) it appears not to be able to inhibit strand annealing (Figure 3.1, *lanes 7, 8 and 9*) as no discernible difference between the shifting of these lanes and those with NC only (Figure 3.1, *lanes 4, 5 and 6*) are detected. Increasing the concentration of Apo3G to 32-fold more than the template RNA does not appear to overcome this (Figure 3.1, *lanes 10, 11 and 12*). The Apo3G monomeric F/W mutant and the Apo3G catalytic mutant, E259Q, also appear to have no effect on NC-mediated $tRNA^{Lys,3}$ strand annealing (data not shown).

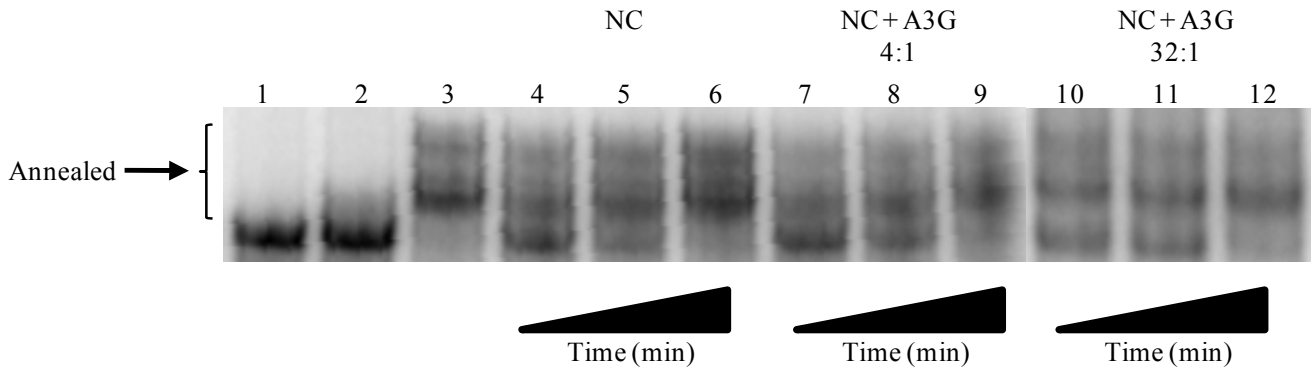

Figure 3.1 **Apo3G does not inhibit Nucleocapsid mediated strand annealing.** Template RNA (104 nt) ^{32}P labeled at the 5'-end was added to reactions at a concentration of 20 nM. NC was added at a concentration to saturate the RNA (85:1, 1700 nM) as it binds 1 NC per 7 nt (Rein et al., 1998). The 4:1 ratio of Apo3G to template RNA (80 nM Apo3G) represents the concentration of Apo3G estimated to be found in a *ΔVif HIV* virion (see Table 2.1). NC alone (*lanes* 4-6) or in the presence of either a 4:1 Apo3G (*lanes* 7-9) or 32:1 ratio of Apo3G to the template RNA (*lanes*10-12) was tested. Samples were taken at 5, 10 and 30 min. Groups of timed assays are denoted with a triangle. Template RNA by itself (*lane* 1) and template RNA with $tRNA^{Lys,3}$, but in the absence of NC (*lane* 2) are negative controls. Lane 3 is with the $tRNA^{Lys,3}$ heat annealed to the template RNA which serves as a positive control.

3.1.2 Determining the minimal concentration of nucleocapsid that can promote annealing of $tRNA^{Lys,3}$ to the primer binding site of HIV RNA

When NC was present at an 85-fold excess to the template RNA, Apo3G at both the 4:1 and 32:1 ratios over the template RNA were both shown to not interfere with NC mediated $tRNA^{Lys,3}$ to the PBS region of the template RNA (Figure 3.1). We hypothesized that lowering the concentration of NC may allow Apo3G to compete better with NC for RNA, therefore allowing Apo3G to prevent NC from facilitating $tRNA^{Lys,3}$ annealing. Titrating the concentration of NC (Figure 3.2) reveals that an NC ratio to the template RNA as low as 21:1 (425 nM) still allows NC to facilitate $tRNA^{Lys,3}$ annealing (Figure 3.2 *lanes 8, 9 and 10).*

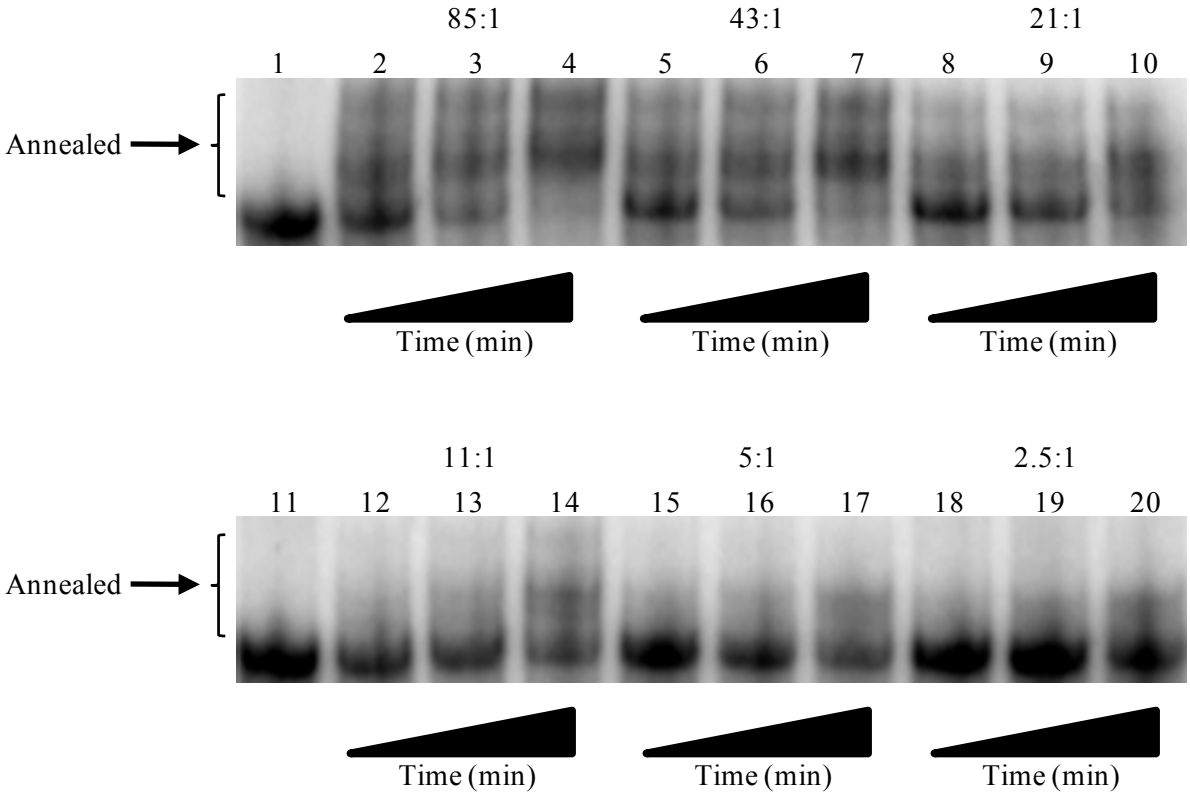

Figure 3.2 **Titration of nucleocapsid concentration.** Template RNA (104 nt) ^{32}P-labeled at the 5'-end was added to reactions at a concentration of 20 nM. NC was added to the reactions at ratios to the template RNA of 85:1 (*lanes* 2-4), 43:1 (*lanes* 5-7), 21:1 (*lanes* 8-10), 11:1 (*lanes* 12-14), 5:1 (*lanes* 15-17) and 2.5:1 (*lanes* 18-20). Template RNA by itself (*Lane* 1 and 11) serves as a negative control. Samples were taken at 5, 10 and 30 min. Groups of timed assays are denoted with a triangle.

3.1.3 Nucleocapsid-mediated annealing of $tRNA^{Lys,3}$ to the primer binding site of HIV RNA in the presence of native and mutant APOBEC3G

Using the ratio of 21:1 NC to template RNA determined from Figure 3.2 to be the lowest concentration of NC that could facilitate $tRNA^{Lys,3}$ annealing, a 4:1 ratio of Apo3G (native and mutants) to template RNA were added to the annealing assay reactions (Figure 3.3). This method was chosen to assess whether or not having protein concentrations in favor of Apo3G inhibition (higher Apo3G and lower NC concentrations) would better enable Apo3G to inhibit NC mediated $tRNA^{Lys,3}$ annealing to the PBS region. The radiolabelled template RNA by itself migrated as a single band, which served as a negative control (Figure 3.3 *lane 1*). The NC alone was able to facilitate $tRNA^{Lys,3}$ annealing to the PBS region as evidenced by the upward band shift (Figure 3.3 *lanes* 16, 17 and 18) as

shown previously in Figure 3.2 (*lanes* 8, 9 and 10*)*. However adding a 4-fold excess to the template RNA of either native (Figure 3.3 *lanes* 3, 4 and 5), F/W mutant (Figure 3.3 *lanes* 6, 7 and 8), E259Q (Figure 3.3 *lanes* 10, 11 and 12) or the clinical H186R mutant (Figure 3.3 *lanes* 13, 14 and 15) did not result in the inhibition of NC mediated strand annealing of the $tRNA^{Lys,3}$. From this it can be concluded that it is unlikely that Apo3G nor any of the mutants used in this study inhibit NC mediated of $tRNA^{Lys,3}$. This appears to be the case regardless of either Apo3G or NC concentration.

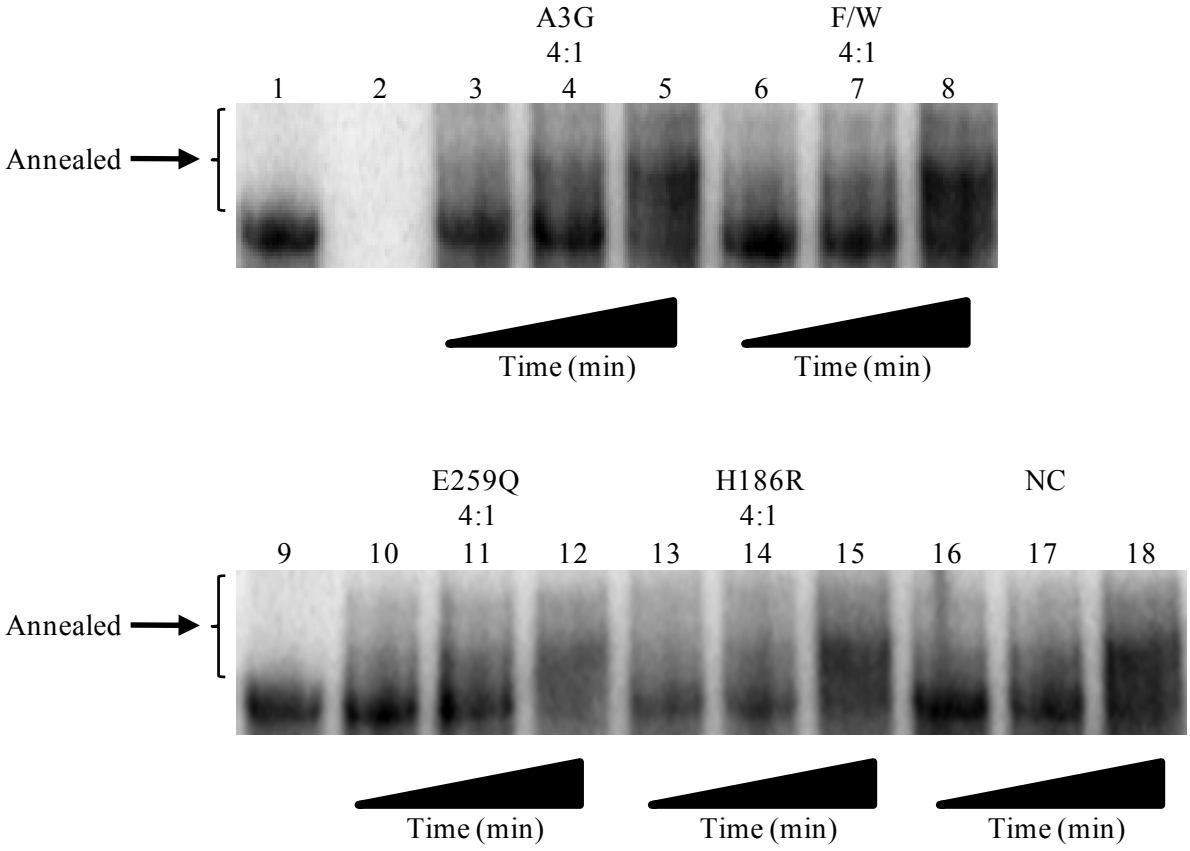

Figure 3.3 **APOBEC3G does not inhibit NC mediated strand annealing when the concentration of NC is low.** Template RNA (104 nt) ^{32}P-labeled at the 5'-end was added to reactions at a concentration of 20 nM. NC was added to the reactions at a ratio to the template RNA of 21:1. Native Apo3G and mutants were added to the reactions at a ratio to the template RNA of 4:1. NC was added to the reaction in the presence of Apo3G (*lanes* 3-5), F/W mutant (*lanes* 6-8), E259Q (*lanes* 10-12), H186R (*lanes* 13-15). Lanes 1and 9, in which PBS RNA is present alone, serves as a negative control. Lanes 16-18, which are NC alone, serve as a positive control. Samples were taken at 5, 10 and 30 min. Groups of timed assays are denoted with a triangle.

3.1.4 APOBEC3G does not compete with nucleocapsid for template RNA binding

We hypothesized that because both NC and Apo3G can both bind to RNA that they could possibly compete for RNA binding. To determine if Apo3G could compete with NC for RNA binding, and possibly inhibit NC-mediated strand annealing, we used rotational anisotropy to determine the apparent dissociation constant (K_d) of Apo3G and NC for a F-labeled version of the template RNA. Here wanted to assess whether or not prebinding RNA with Apo3G could cause any change in the affinity of NC for RNA and *vice versa*, which would be indicative of Apo3G and NC competing for the RNA substrate.

We prebound specific concentrations of Apo3G to the RNA and then used this as the substrate for NC binding experiments and *vice versa*. Taking into account results of the annealing assay, our hypothesis was that Apo3G and NC would not interfere with each other's binding to the RNA substrate. The apparent K_d values of NC and Apo3G for the RNA were similar (Table 3.1, 402 and 383 nM, respectively). Prebinding of the template RNA with either a 10: 1 (500 nM) or 17:1 (850 nM) ratio of Apo3G to the template RNA did not result in a significant difference in the apparent K_d of NC (Table 3.1, 368 and 441nM, respectively). Similarly, prebinding the template RNA with either a 10: 1 or 17:1 ratio of NC did not result in a significant difference in the apparent K_d of Apo3G (Table 3.1, 501 and 489 nM, respectively). It is therefore unlikely that Apo3G competes with NC for RNA binding. This data is congruous with the annealing assay data which also suggests that Apo3G does not interfere with NC mediated strand annealing (Figures 3.1 and 3.3).

Table 3.1 **Apparent dissociation constants (K_d) of native APOBEC3G and nucleocapsid with for template RNA.** The K_d values shown are for Apo3G and nucleocapsid individually, or with either 500 nM or 850 nM Apo3G or nucleocapsid prebound to the template PBS RNA.

Nucleocapsid prebound to RNA (nM)	Apo3G Kd (nM)	Apo3G prebound to RNA (nM)	Nucleocapsid Kd (nM)
0	383 ± 205	0	402 ± 209
500	501 ± 1	500	368 ± 149
850	489 ± 42	850	441 ± 47

3.2 APOBEC3G inhibition of reverse transcriptase-mediated polymerization on an RNA/RNA primer/template

3.2.1 APOBEC3G inhibits reverse transcriptase-mediated primer extension

As Apo3G has a strong affinity for ssRNA ((Chelico et al., 2010) and Table 3.1), we hypothesized that Apo3G could inhibit RT mediated primer extension by either physically blocking RT from adding nucleotides or by competing with RT for RNA binding. To establish the degree of inhibition of RT-mediated DNA synthesis by Apo3G we analyzed (-) DNA primer extension activity. For the assay we heat annealed a synthetic RNA primer in lieu of the $tRNA^{Lys,3}$ to the template RNA and assayed the products by gel electrophoresis (Figure 3.4, sketch). This is a model system for (-) DNA primer extension synthesis (Figure 1.2). RT is able to extend ~70% of the primer and 5% of these products result in full length transcripts (Figure 3.4 A). When Apo3G was added to the primer extension reaction at a 4-fold ratio over the primer/template, which is the estimated concentration in a *ΔVif* HIV virion (see Section 2.0), we observed a decrease in the efficiency of primer extension (Figure 3.4 B, 4:1). The total amount of primer initiation that is inhibited in the presence of Apo3G ranges from 2.4-fold (2.5 min) to 1.5-fold (60 min) (compare Figure 3.4 B and Figure 3.4 A). Apo3G also changes the population of extension products and amount of fully extended primer. Apo3G prevents the majority of primer from being elongated past ~ 12 nt (compare Figure 3.4 B and Figure 3.4 A). Most notably, the presence of Apo3G (4:1, Figure 3.4 B) is able to decrease the amount of fully extended primer by 30-fold in comparison to primer extension by RT (Figure 3.8). Addition of greater amounts of Apo3G (32:1, Figure 3.4 C) resulted in almost the same amount of total primer extension as Apo3G (4:1, Figure 3.4 B) with percent primer extension reaching 34% and 47% at 60 min, respectively. However, the final extension product for the assay on which 32:1 ratio of Apo3G: primer/template used by analyzing integrated gel band intensities was not detectable (Figure 3.4 C and Figure 3.8). These results suggest that on an RNA/RNA primer/template, Apo3G primarily impacts primer elongation and the ability of RT to synthesize full length transcripts, but can also inhibit RT by preventing primer initiation perhaps by blocking RT from accessing the primer template junction.

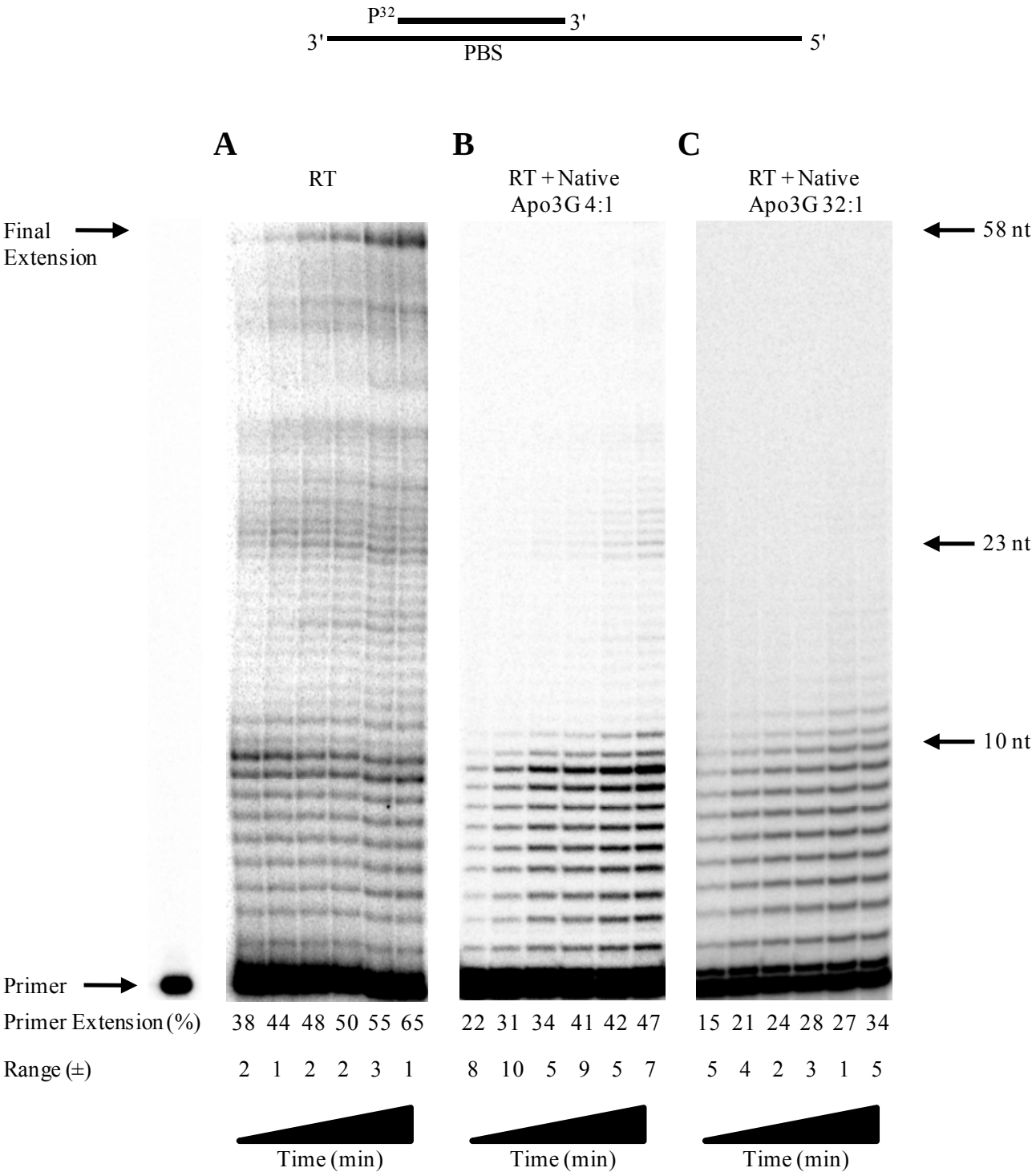
P32
3'
3'
5'
PBS
A
B
C
RT
RT + Native Apo3G 4:1
RT + Native Apo3G 32:1
Final Extension
58 nt
23 nt
10 nt
Primer
Primer Extension (%)
38 44 48 50 55 65
22 31 34 41 42 47
15 21 24 28 27 34
Range (±)
2 1 2 2 3 1
8 10 5 9 5 7
5 4 2 3 1 5
Time (min)
Time (min)
Time (min)

Figure 3.4 **Reverse transcriptase-mediated primer extension in the absence and presence of native APOBEC3G.** A ^{32}P-labeled RNA primer was heat annealed to a 104 nt template RNA containing the PBS (*sketch)*. Complete extension of the primer results in a DNA of 58 nt. (A) primer extension by RT. (B-C) primer extension by RT in the presence of either a 4:1 (B) or 32:1 (C) ratio of native Apo3G to the primer/template. The primer/template concentration was 20 nM. The 4:1 ratio of Apo3G to primer/template (B, 80 nM Apo3G) represents the concentration of Apo3G estimated to be found in a *ΔVif HIV virion (see Section 2.0).* Samples were collected at the following times: 2.5, 5, 10, 15, 30 and 60 min. Total primer extension (%) averaged from two independent trials and the range (±) of the data is shown below gels.

3.2.2 Oligomerization facilitates APOBEC3G inhibition of reverse transcriptase mediated primer extension

We hypothesized that oligomerization may be important for Apo3G inhibition of RT mediated primer extension. Being able to form higher order structures likely enables Apo3G to block RT primer extension activity. Based on our hypothesis, if Apo3G were to lose this ability, we predicted that Apo3G inhibition of RT mediated primer extension activity would be at a deficit. We chose to use the Apo3G F/W mutant to assess whether or not oligomerization is important for RT inhibition. The Apo3G F/W mutant has been shown to exist as a monomer in solution and when bound to DNA or RNA (Chelico et al., 2010; Huthoff et al., 2009).

Under the same conditions used for native Apo3G, we tested if the F/W mutant could inhibit RT-mediated primer extension (Figure. 3.5). The F/W mutant was found to inhibit RT-mediated primer initiation to the same extent as native Apo3G (compare Figure 3.4 B and Figure 3.5 A, Primer extension (%)). However, in the presence of the F/W mutant, RT is able to undergo primer elongation past ~12 nt (Figure 3.5 A), similar to extension in the absence of native Apo3G (Figure 3.4 A). The F/W mutant inhibits RT-mediated synthesis of full length products by only 1.3-fold, which is less than Native Apo3G (Figure 3.8). Upon increasing the concentration of the F/W mutant, the final extension products formed by RT are inhibited more than at the lower concentration (Figure 3.8 and compare Figure 3.5 B and Figure 3.5 A), demonstrating that the deficiency of the F/W mutant to inhibit RT primer extension can be partially recovered by increasing the enzyme concentration. However, all together the results indicate that the absence of oligomerization hinders the ability of Apo3G to inhibit RT-mediated primer extension.

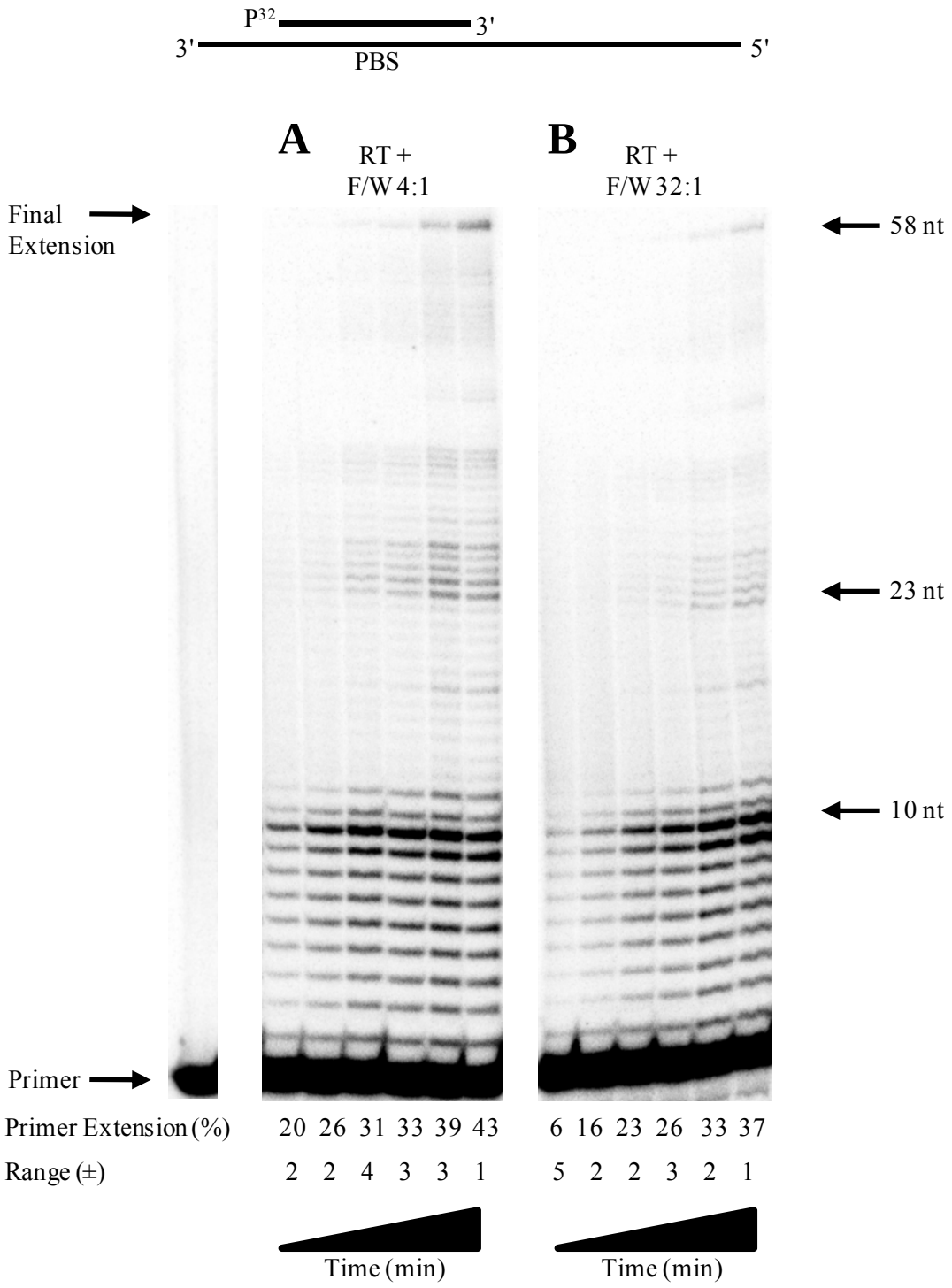
P32
3'
3'
5'
PBS
A
RT +
F/W 4:1
B
RT +
F/W 32:1
Final
Extension
58 nt
23 nt
10 nt
Primer
Primer Extension (%)
20 26 31 33 39 43
6 16 23 26 33 37
Range (±)
2 2 4 3 3 1
5 2 2 3 2 1
Time (min)
Time (min)

Figure 3.5 **Impaired inhibition of reverse transcriptase-mediated primer extension by the monomeric F/W mutant.** A ^{32}P-labeled RNA primer was heat annealed to a 104 nt RNA template containing the PBS (*sketch)*. Complete extension of the primer results in a DNA of 58 nt. (A-B) primer extension by RT in the presence of either a 4:1 (A) or 32:1 (B) ratio of F/W mutant to the primer/template. The primer template concentration was 20 nM. Samples were collected at the following times: 2.5, 5, 10, 15, 30 and 60 min. Total primer extension (%) averaged from two independent trials and the range (±) of the data is shown below gels.

3.2.3 Inhibition of reverse transcriptase-mediated primer extension by the catalytic mutant E259Q

We hypothesized that in addition to losing the ability to deaminate, that the Apo3G E259Q deamination mutant may also be defective in its ability to inhibit RT mediate primer extension. This hypothesis is based on the presumption that this mutation, in addition to abrogating the ability of Apo3G to deaminate ssDNA, may also cause structural changes that could alter its ability to inhibit RT mediated primer extension. This would therefore account for its deficiency to inhibit HIV infectivity found in other studies (Bishop et al., 2008; Mbisa et al., 2007; Miyagi et al., 2007; Schumacher et al., 2008).

The E259Q mutant is able to decrease the efficiency of RT-mediated primer extension (Figure 3.6 A). The primer initiation by RT is decreased 2.5-fold (2.5 min) to 1.6-fold (60 min) in the presence of E259Q, similar to native Apo3G (compare Figure 3.6 A and Figure 3.4 B). In contrast to native Apo3G, the E259Q mutant only causes a 4-fold decrease in the amount of final extension product (58 nt, Figure 3.6 A and Figure 3.8) compared to a 30-fold decrease with native Apo3G (Figure 3.4 B and Figure 3.8). At a higher concentration of E259Q the inhibition of primer initiation is similar to native Apo3G (32:1, compare Figure 3.6 B and Figure 3.4 C), but fully extended products are detectable whereas they were not with native Apo3G (Figure 3.8).

The E259Q mutant is therefore able to reduce the efficiency of RT-mediated primer extension in a similar fashion to native Apo3G. However that the ability of E259Q to prevent the formation of final extension products is diminished relative to native Apo3G suggesting that the E259Q mutant is fundamentally different than native Apo3G beyond its ability to deaminate. This indicates that this mutation may cause more than just a loss in the ability to deaminate making it poor proxy for Native Apo3G.

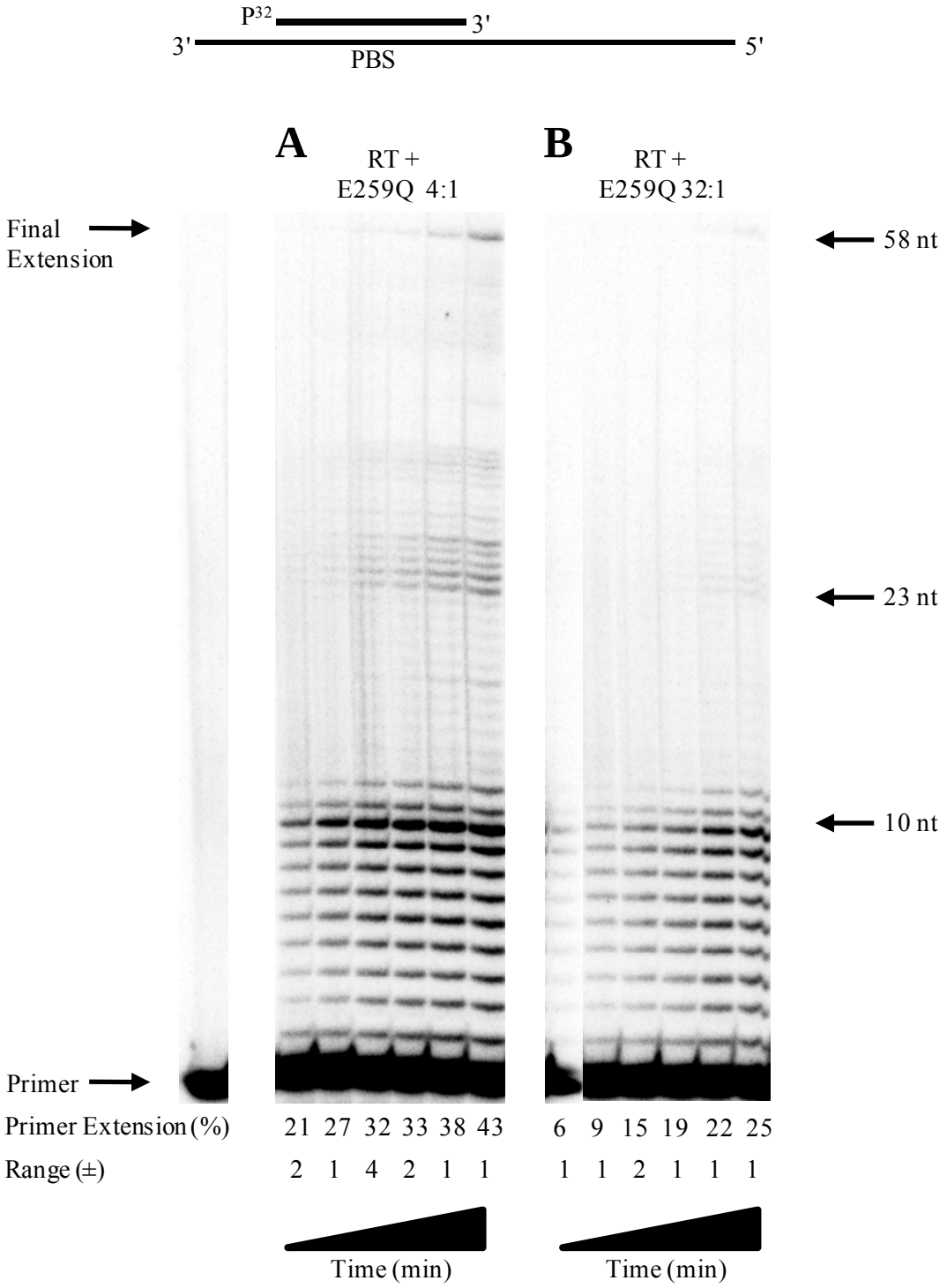
P32
3'
3'
5'
PBS
A
RT +
E259Q 4:1
B
RT +
E259Q 32:1
Final
Extension
58 nt
23 nt
10 nt
Primer
Primer Extension (%)
21 27 32 33 38 43
6 9 15 19 22 25
Range (±)
2 1 4 2 1 1
1 1 2 1 1 1
Time (min)
Time (min)

Figure 3.6 **The catalytic mutant E259Q inhibits reverse transcriptase-mediated primer extension.** A ^{32}P-labeled RNA primer was heat annealed to a 104 nt template RNA containing the PBS (*sketch)*. Complete extension of the primer results in a DNA of 58 nt. (A-B) primer extension by RT in the presence of either a 4:1 (A) or 32:1 (B) ratio of E259Q to the primer/template. The primer/template concentration was 20 nM. Samples were collected at the following times: 2.5, 5, 10, 15, 30 and 60 min. Total primer extension (%) averaged from two independent trials and the range (±) of the data is shown below gels.

3.2.4 Inhibition of reverse transcriptase-mediated primer extension by the clinical mutant H186R

The Apo3G H186R clinical mutant is associated with HIV patients whose infection quickly progresses to AIDS (An et al., 2004). We hypothesized that the diminished ability to restrict HIV infection of patients that harbour the Apo3G H186R mutation may be attributed to a reduced capacity to inhibit RT primer extension.

The H186R clinical mutant can inhibit RT mediated primer extension. Its ability to inhibit overall primer extension is similar to Apo3G (*compare primer extension (%),* Figure 3.4 B,C and Figure 3.7). The H186R mutant is less able to inhibit the formation of final extension products mediated by RT as compared to Apo3G when present at a ratio of 4:1 enzyme: primer/template (Figure 3.8). However, the native and H186R Apo3G forms exhibit similar inhibition of the final extension product formation at a ratio of enzyme to the primer/template of 32:1 (Figure 3.8).

The Apo3G H186R mutant is able to restrict total and final extension products in a similar manner to Native Apo3G. It is therefore unlikely that patients with the Apo3G H186R mutation have a reduced ability to inhibit RT mediated primer extension.

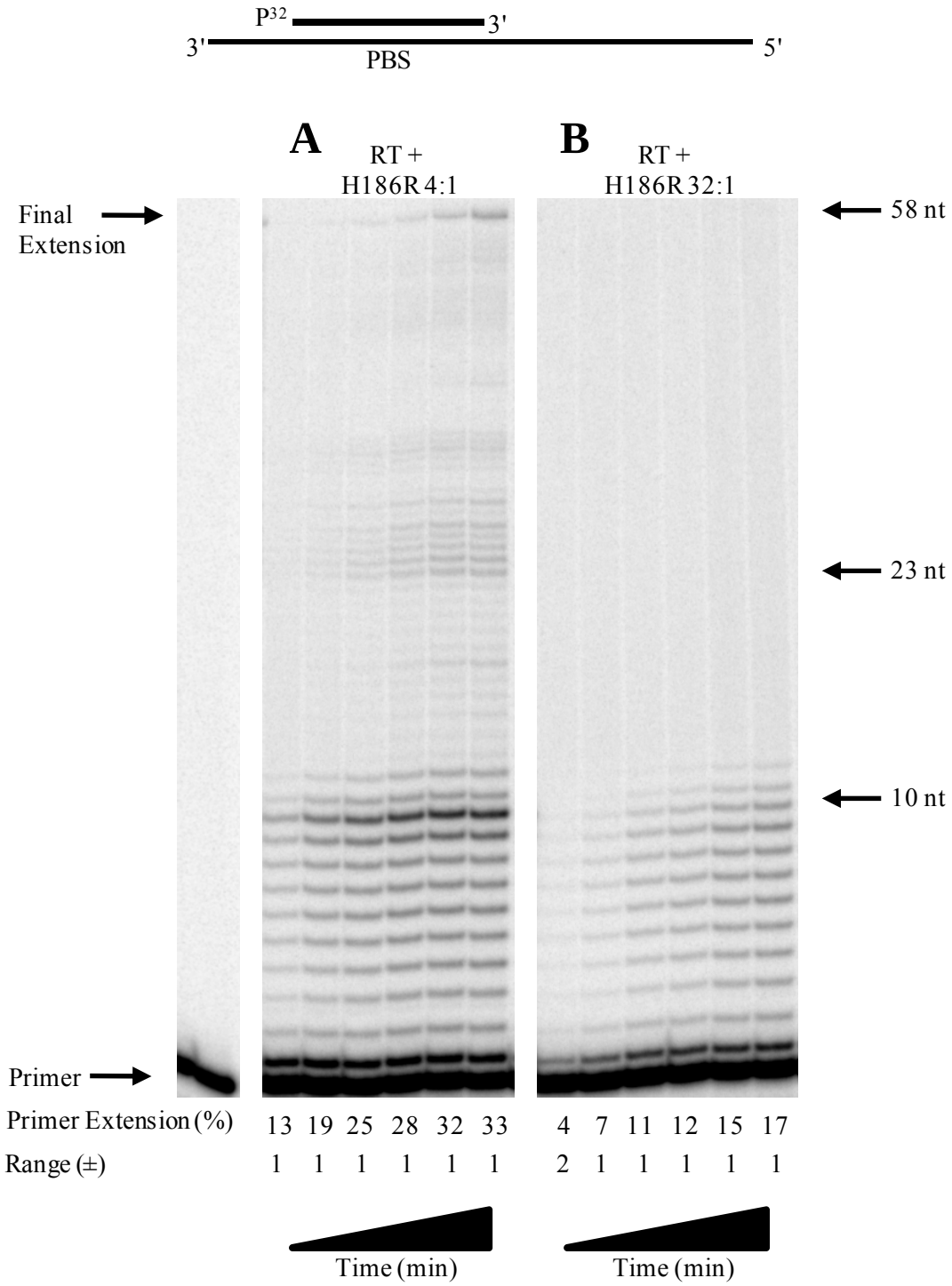
P32
3'
3'
5'
PBS
A
RT +
H186R 4:1
B
RT +
H186R 32:1
Final
Extension
58 nt
23 nt
10 nt
Primer
Primer Extension (%)
13 19 25 28 32 33
4 7 11 12 15 17
Range (±)
1 1 1 1 1 1
2 1 1 1 1 1
Time (min)
Time (min)

Figure 3.7 **The clinical mutant H186R inhibits reverse transcriptase-mediated primer extension.** A ^{32}P-labeled RNA primer was heat annealed to a 104 nt template RNA containing the PBS (*sketch)*. Complete extension of the primer results in a DNA of 58 nt. (A-B) primer extension by RT in the presence of either a 4:1 (A) or 32:1 (B) ratio of H186R to the primer/template. The primer/template concentration was 20 nM. Samples were collected at the following times: 2.5, 5, 10, 15, 30 and 60 min. Total primer extension (%) averaged from two independent trials and the range (±) of the data is shown below gels.

3.2.5 Synthesis of full length reverse transcripts by reverse transcriptase in the absence and presence of native and mutant APOBEC3G

In addition to quantifying the overall primer extension, we examined the type of inhibition of primer extension products RT produced in the presence of the Apo3G forms. When looking at the distribution of the final extension product bands, Apo3G at a concentration of 80 nM and with the primer template concentration of 20 nM (4:1 ratio), the ratio found in HIV virions when Vif is not present (Xu et al., 2007), can significantly reduce the quantity of the final extension product. The quantity of final extension bands seen with no Apo3G present is 5% of the total extension products (Figure 3.8 A, *Native, 4:1* and Figure 3.4 *B lane 6*), as compared to when there is no Apo3G present which results in the final extension products being made to 0.2% of the total extension products (Figure 3.8, *RT* and Figure 3.4 *A*, *RT*). At the 4:1 ratio, there is a decrease in the final extension product from RT alone for reactions in the presence of native Apo3G, F/W mutant, E259Q and H186R. When the F/W mutant, E259Q, or H186R are used, we see that their ability to reduce the quantity of final extension products in the final band is less than native Apo3G (Figure 3.8, 4:1; Figure 3.5 *A lane 6*, Figure 3.6 *A lane 6* and Figure 3.7 *A lane 6,* respectively).

This trend is also followed when the Apo3G native and mutant proteins are added at higher ratio (32:1) to the primer/ template (Figure 3.8 and 3.4 *C*). At the 32:1 ratio, the final extension product band of Apo3G is not detectable on the gel. The quantity of final extension product band from reactions with the F/W mutant (Figure 3.8A, 1.4%), E259Q (Figure 3.8 A, 0.5%), and H186R (Figure 3.8A, 0.1%) are less than at the lower concentration, but the F/W and E259Q mutants still inhibit the accumulation of reverse transcripts less than native Apo3G.

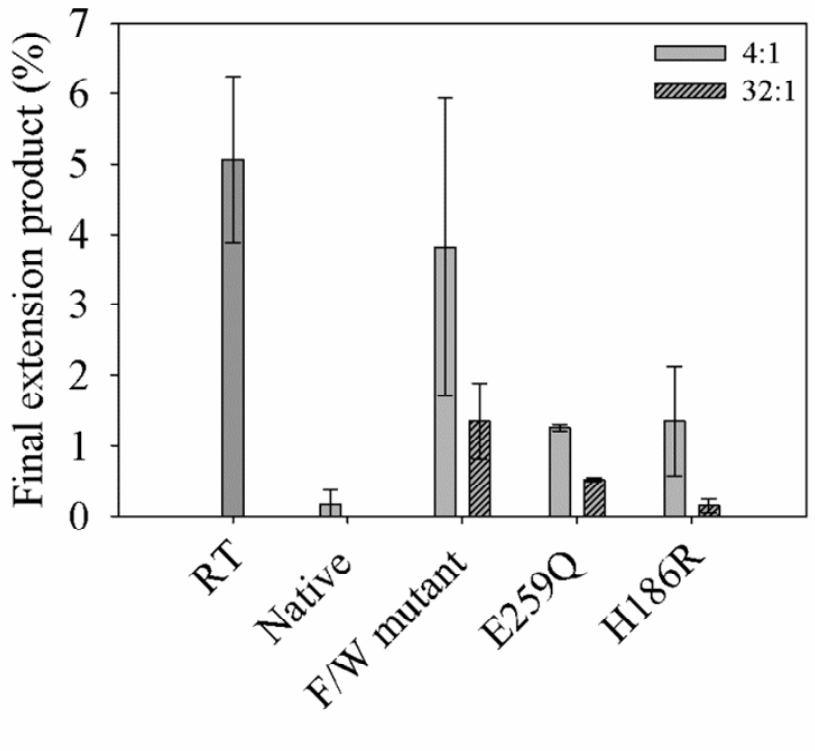

Figure 3.8 **Synthesis of full length reverse transcripts by reverse transcriptase in the absence and presence of native and mutant APOBEC3G.** *A*, Comparison of normalized percent final extension product (58 nt) of RT in the absence or presence of a 4:1 or 32:1 ratio of native Apo3G, F/W mutant, E259Q or H186R to the primer/template. The primer/template concentration was 20 nM. The 4:1 ratio of Apo3G to primer/template (80 nM) represents the concentration of Apo3G estimated to be found in a *ΔVif HIV* virion. The final extension product value has been normalized to the total primer extension of RT. The percent final extension product for native Apo3G 32:1 ratio could not be calculated since there was no detectable band from gel assays. Data is summarized from analysis of the 60 min sample from experiments shown in Figure 3.4-3.7. The data shown is from two independent trials and the range of the data is based on the standard deviation between the two trials (error bars).

3.2.6 Binding affinity of APOBEC3G forms for the primer/template correlates with the ability to inhibit reverse transcriptase

We hypothesized that the difference in the ability of native Apo3G and the mutants (F/W and E259Q) to inhibit RT-mediated primer extension may be attributed to their binding affinity for primer/template RNA. Additionally, we hypothesized that if Apo3G had a stronger affinity for the primer/template that it could possibly compete with RT for binding to the primer/template.

We therefore used fluorescence depolarization (rotational anisotropy) to determine the apparent K_d of native and mutant Apo3G and RT for the primer/template. Native Apo3G binds the primer template with ~3-fold greater affinity than RT (Table 3.2, K_d of 192 and 549 nM, respectively). The Apo3G mutants both bind the primer template with less affinity than native Apo3G and have K_d values that are more similar to RT (Table 3.2, F/W mutant, 354 nM; E259Q, 477 nM). The binding data demonstrates that E259Q cannot be used interchangeably with native Apo3G when a deamination-null mutant is required because the binding affinities for the template differ by 2.5- fold.

The data suggest that binding affinity for RNA may contribute to the ability of Apo3G to inhibit synthesis of reverse transcripts since the F/W mutant and E259Q which inhibit RT-mediated DNA synthesis less than native Apo3G (Figure 3.8), even at the 32:1 ratio, also bind the primer/template with less affinity. Also it is suggested that Apo3G could compete with RT for primer/template binding as a substrate as the apparent K_d of native Apo3G for the primer/template is less than the apparent K_d of RT for the primer/template

Table 3.2 **Apparent dissociation constants (K_d) of reverse transcriptase and native and mutant APOBEC3G.**

Enzyme	**K_d (nM)**
native Apo3G	192 ± 39
F/W mutant	354 ± 26
E259Q	477 ± 69
RT	549 ± 42

3.2.7 Combined binding of reverse transcriptase and APOBEC3G to primer/template RNA

As an indication of whether the higher binding affinity for the primer/template of native Apo3G decreased the ability of RT to bind the primer/template, we used electrophoretic mobility shift assays where RT competed for primer/template from prebound Apo3G. The RT alone can saturate the primer/template when a 25-fold excess of RT to primer/template is added (Figure 3.9 B, *lane 7, 1240 nM*). We tested whether prebinding a 10-fold excess of Apo3G to the primer/template would increase the amount of RT needed to saturate the primer/template. If RT binding to the primer/template is not affected by the presence of native Apo3G we would expect that the RT would still be able to saturate the substrate. Because the Apo3G added as a competitor is able to shift 35% of the substrate (Figure 3.9 C, *lane 2*) we expect that all the substrate should be shifted with less RT. Figure 3.9C shows that RT is not prevented from binding to the primer/template and can saturate the primer/template at ~620 nM, rather than at 1240 nM (Figure 3.9 C, *lanes 8 and 9*). The E259Q and the F/W mutant were also found to not affect the ability of RT to bind the primer/template (Figure 3.9 D and Figure 3.9 E, respectively). The ability of both Apo3G and RT to bind the primer/template may be because the RT preferentially binds at the primer/template junction, whereas Apo3G can bind anywhere along the RNA molecule.

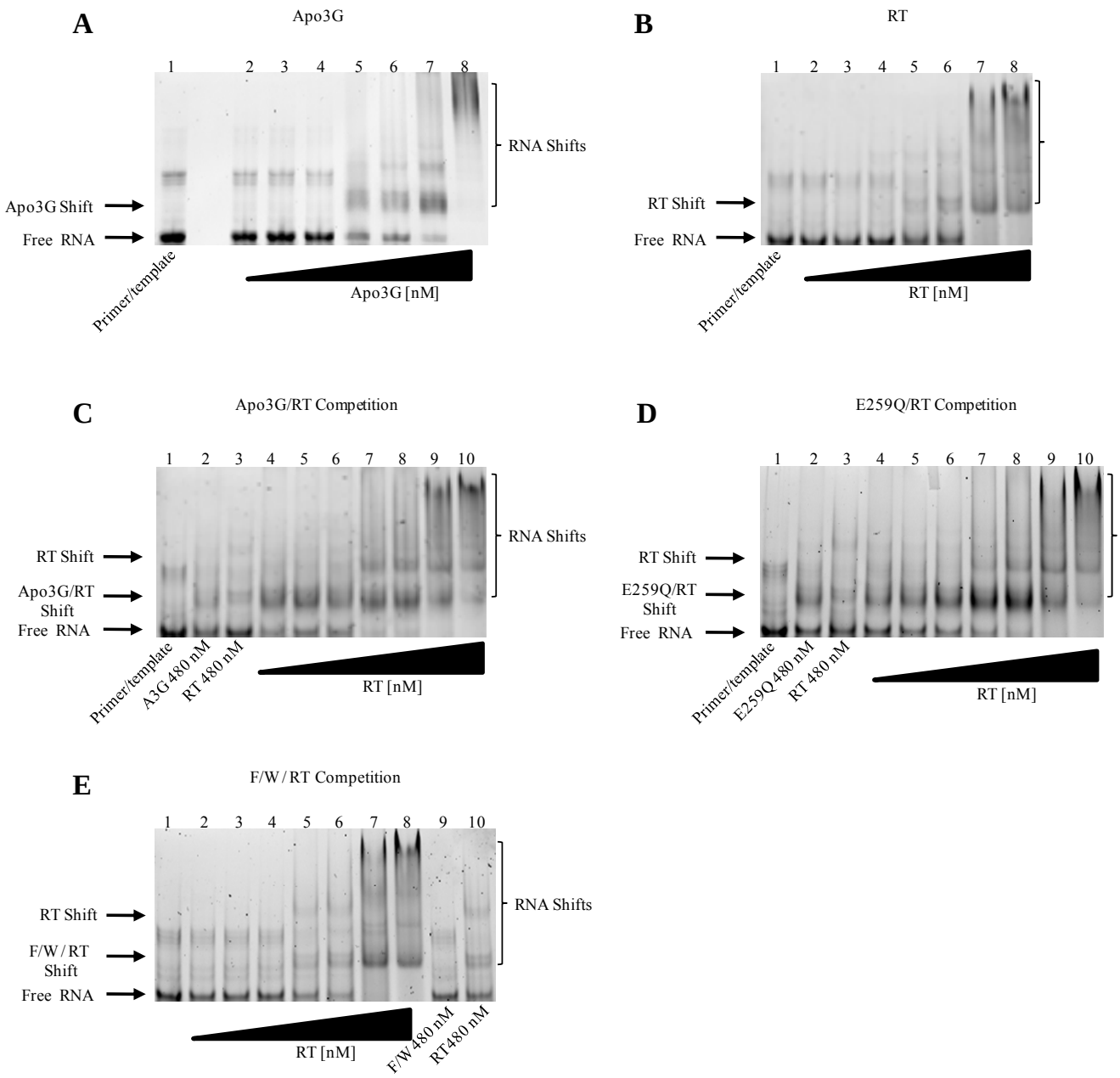
A
Apo3G
1 2 3 4 5 6 7 8
RNA Shifts
Apo3G Shift
Free RNA
Primer/template
Apo3G [nM]
B
RT
1 2 3 4 5 6 7 8
RT Shift
Free RNA
Primer/template
RT [nM]
C
Apo3G/RT Competition
1 2 3 4 5 6 7 8 9 10
RNA Shifts
RT Shift
Apo3G/RT Shift
Free RNA
Primer/template
A3G 480 nM
RT 480 nM
RT [nM]
D
E259Q/RT Competition
1 2 3 4 5 6 7 8 9 10
RT Shift
E259Q/RT Shift
Free RNA
Primer/template
E259Q 480 nM
RT 480 nM
RT [nM]
E
F/W / RT Competition
1 2 3 4 5 6 7 8 9 10
RNA Shifts
RT Shift
F/W / RT Shift
Free RNA
RT [nM]
F/W 480 nM
RT 480 nM

Figure 3.9 **Visualization of combined binding of native APOBEC3G and reverse transcriptase to the primer/template using an electrophoretic mobility shift assay.** (A-B) Apo3G (A) or RT (B) was titrated into sample reactions containing 50 nM fluorescein (F)-labelled primer/template at concentrations of 60, 120, 240, 480, 620, 1240 and 2480 nM. (C-E) RT was titrated into sample reactions containing 50 nM fluorescein (F)-labelled primer/template at concentrations of 60, 120, 240, 480, 620, 1240 and 2480 nM with 480 nM native Apo3G (C), 480 nM E259Q (D) or 480 nM F/W mutant (E) prebound to the primer/ template. Free and bound RNA are denoted on gels. (C) shift of prebound Apo3G (*lane* 2, 480 nM) is shown on gel in comparison RT bound alone at 480 nM (*lane* 3) to assist in differentiating the combined Apo3G/RT shift from an RT shift. *D*, shift of prebound E259Q (*lane* 2, 480 nM) is shown on gel in comparison RT bound alone at 480 nM (*lane* 3) to assist in differentiating the combined E259Q/RT shift from an RT shift. *E*, shift of prebound F/W (*lane* 9, 480 nM) is shown on gel in comparison RT bound alone at 480 nM (*lane* 10) to assist in differentiating the combined F/W / RT shift from an RT shift.

3.2.8 Protein-protein interactions between APOBEC3G and reverse transcriptase

We hypothesized that Apo3G could inhibit RT by physically binding to it and preventing it from reverse transcribing –ssRNA into +ssDNA. We chose to use rotational anisotropy to test protein-protein interactions between RT and Apo3G. By using a fluorescein labelled Apo3G (F-Apo3G), we found that Apo3G can interact with F-Apo3G with low affinity (K_d 3.5 μM, Figure 3.10). RT also binds to F-Apo3G with a low affinity (K_d 4 μM, Figure 3.10). As a negative control, we assessed whether the monomeric F/W mutant could interact with native Apo3G. As expected, we found no detectable interaction between F-Apo3G and the F/W mutant (Figure 3.10). This data demonstrates that protein-protein interactions between RT and Apo3G are possible, but not as likely to happen *in vivo* as binding to RNA since the protein concentrations required for RT and Apo3G to interact are in the micromolar range, whereas the affinities for RNA are in the nanomolar range (Table 3.2).

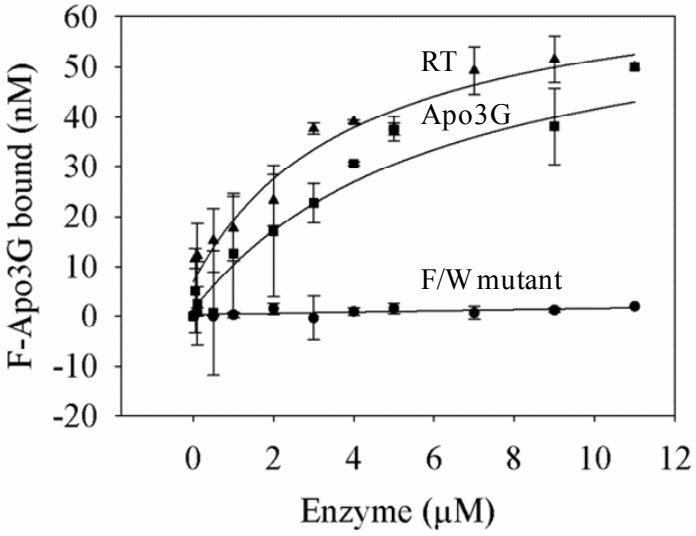

Figure 3.10 **Analysis of interaction between APOBEC3G forms and reverse transcriptase to fluorescently labelled APOBEC3G by steady-state fluorescence depolarization.** Apparent dissociation constants (K_d) were determined by titrating increasing concentrations (*x-axis)* of RT, native Apo3G or F/W mutant to 50 nM of fluorescein (F)-labelled native Apo3G. RT binds F-Apo3G with an apparent Kd of 4 μM, which is similar to the apparent K_d of native Apo3G and F-Apo3G (3.5 μM).

3.2.9 Using pyrrolo-C to detect protein induced conformational changes in primer/template RNA

Previously, native Apo3G has been shown to cause a change in the structure of ssDNA, based on monitoring changes in pyrollo-dC fluorescence (Chelico et al., 2008). Pyrollo-dC is a fluorescent nucleotide analogue that can be used to monitor changes in the local structure of the ssDNA. An increase in fluorescence of the pyrollo-dC is interpreted to mean that a change in the structure of the ssDNA such as bending or wrapping has occurred. We tested a parallel situation with pyrollo-C embedded in RNA. We found that both native and E259Q Apo3G were unable to cause a change in pyrollo-C fluorescence (Figure 3.11). The F/W mutant was able to cause a 2.5-fold change in the pyrollo-C fluorescence (Figure 3.11). Since the F/W mutant displayed the least inhibition of RT-mediated DNA synthesis, the results suggest that changing the structure of the RNA is not a factor in the mechanism by which Apo3G limits synthesis of DNA by RT.

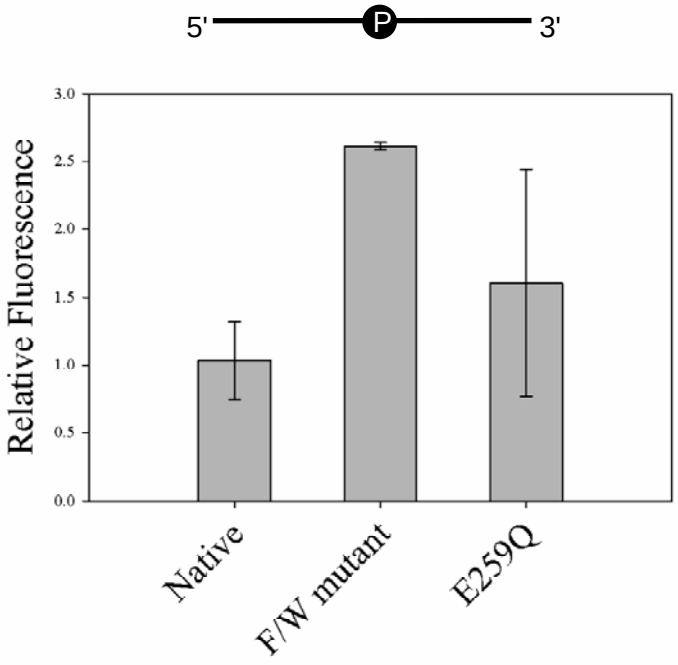

Figure 3.11 **Conformational modulation of RNA by reverse transcriptase and APOBEC3G.** Fluorescence emissions of 100 nM pyrrolo-C labelled RNA (*sketch)* were monitored after the addition of 1.2 μM enzyme. Emissions are plotted as fluorescence value relative to RNA alone (value of 1.0) for native Apo3G, E259Q and F/W mutant. The data show that the F/W mutant is able to cause a 2.5-fold increase in the relative fluorescence of pyrrolo-C, indicating that the structure of the RNA is altered by F/W mutant binding. Native Apo3G and E259Q are not able to cause a significant change in pyrrolo-C fluorescence. Data is from two independent trials and the range of the data is shown.

3.3 RNAseH activity

RT utilizes an RNAseH domain to degrade template RNA during HIV reverse transcription. We hypothesized that if Apo3G could bind RT through a protein-protein interaction it could inhibit RNAseH activity of RT. Since Apo3G does not bind RNA/DNA hybrids with high affinity (Iwatani et al., 2006), it is unlikely that Apo3G can inhibit RNAseH activity through binding nucleic acids and physically blocking RT. With the results from the protein-protein anisotropy (Figure 3.10), we hypothesized that Apo3G could not inhibit RNAseH activity. We tested the RNAseH activity of RT using two methods.

3.3.1 The analysis of RNAseH activity during primer/template extension in the absence and presence of APOBEC3G

The first RNAseH assay employs a ^{32}P-labelled PBS template RNA that is annealed to an unextended RNA primer to form the primer/template such as that used for experiments described in Section 3.2. In this assay, degradation can only take place once the RNA/DNA hybrid is formed by RT-mediated DNA synthesis. Therefore, we do not expect to see 100% RNA degradation based on results from primer extension assays (Figure 3.8). When RT is present alone, RNA degradation is detected (Figure 3.12 A). However when Apo3G is present at a 4:1 ratio to the primer/template, a reduction in the quantity of RNA degradation is observed (Figure 3.12 B). The addition of the Apo3G monomeric mutant F126A/W127A does not appear to result in a reduction in RNA degradation (Figure 3.12 C). More similar to native Apo3G, when the deamination mutant E259Q and the clinical mutant H186R are used, there is minimal RNA degradation (Figure 3.12 D and E, respectively). The presence of Apo3G forms that inhibit synthesis of final extension products the greatest (Figure 3.8) correlated with inhibition of RNAseH activity. Since the RNAseH activity requires a DNA/RNA hybrid, Apo3G appears to be inhibiting RNAseH activity indirectly (Figure 3.12).

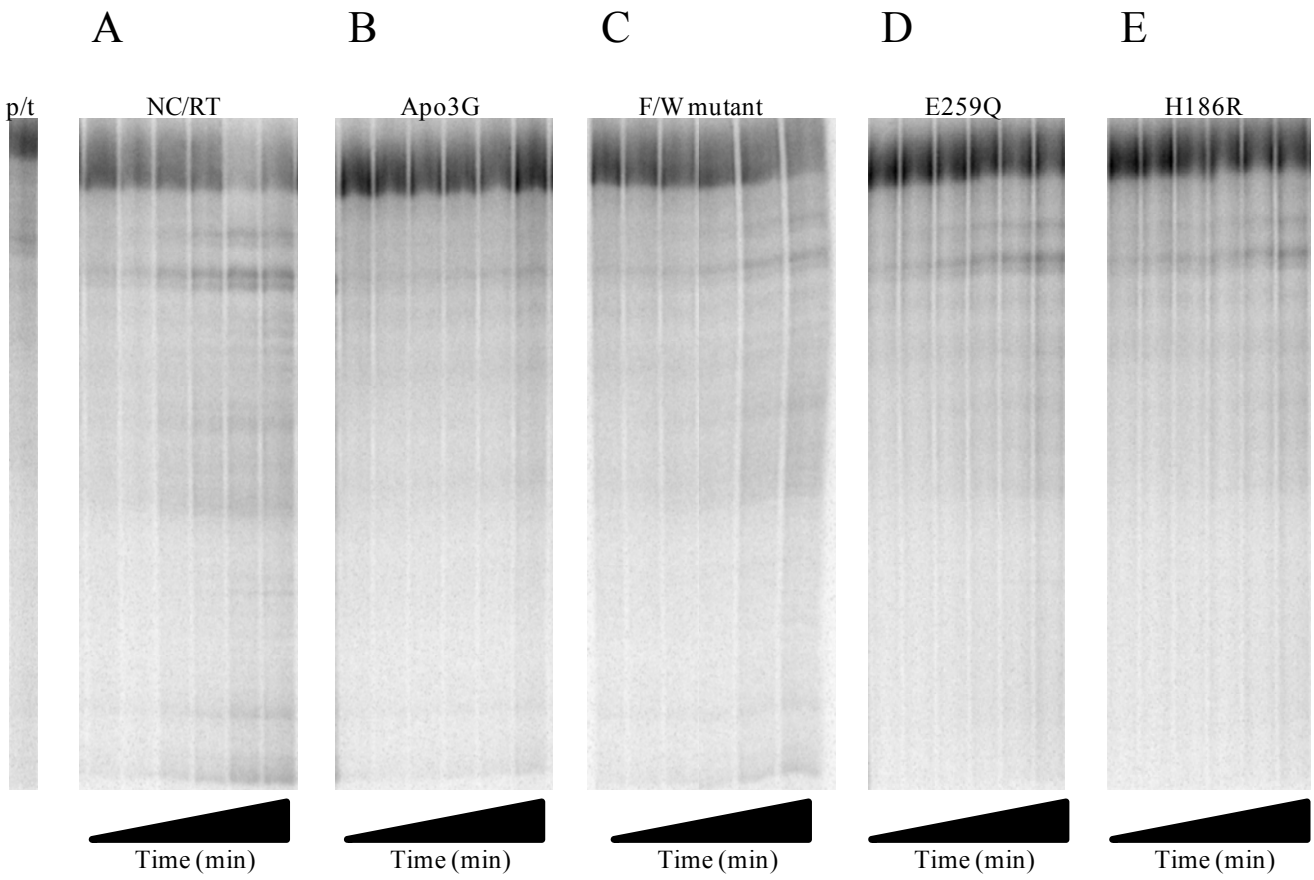

Figure 3.12 **Measurement of RNAseH activity during primer extension.** Reactions contained ^{32}P-labelled template RNA annealed to an unextended RNA primer to form the primer/template. The primer/template was added at 20 nM in the presence of RT buffer, NC (350 nM) and RT (960 nM). RNAseH activity was measured by degradation of the RNA in the absence (A), or presence of a 4-fold excess to the primer/template (80 nM) of native Apo3G (B), F/W mutant (C), E259Q (D) or H186R (E). Samples were taken at 2.5, 5, 10, 15, 30 and 60 min. The single lane by itself (left) shows the unreacted primer/template (p/t) as a negative control.

3.3.2 The analysis of RNAseH activity using a RNA/DNA hybrid in the absence and presence of APOBEC3G

In a second RNAseH assay, we annealed a full complement DNA strand to the ^{32}P-labelled RNA template. In this type of assay, we start with the RNAseH substrate fully available and expect to obtain 100% cleavage of the template RNA. The DNA/RNA hybrid substrate shows significant degradation by RT, as expected (Figure 3.13 A). None of the Apo3G forms at either the low (4:1) or

high (32:1) ratios to the primer/template inhibited RNAseH-mediated RNA degradation.

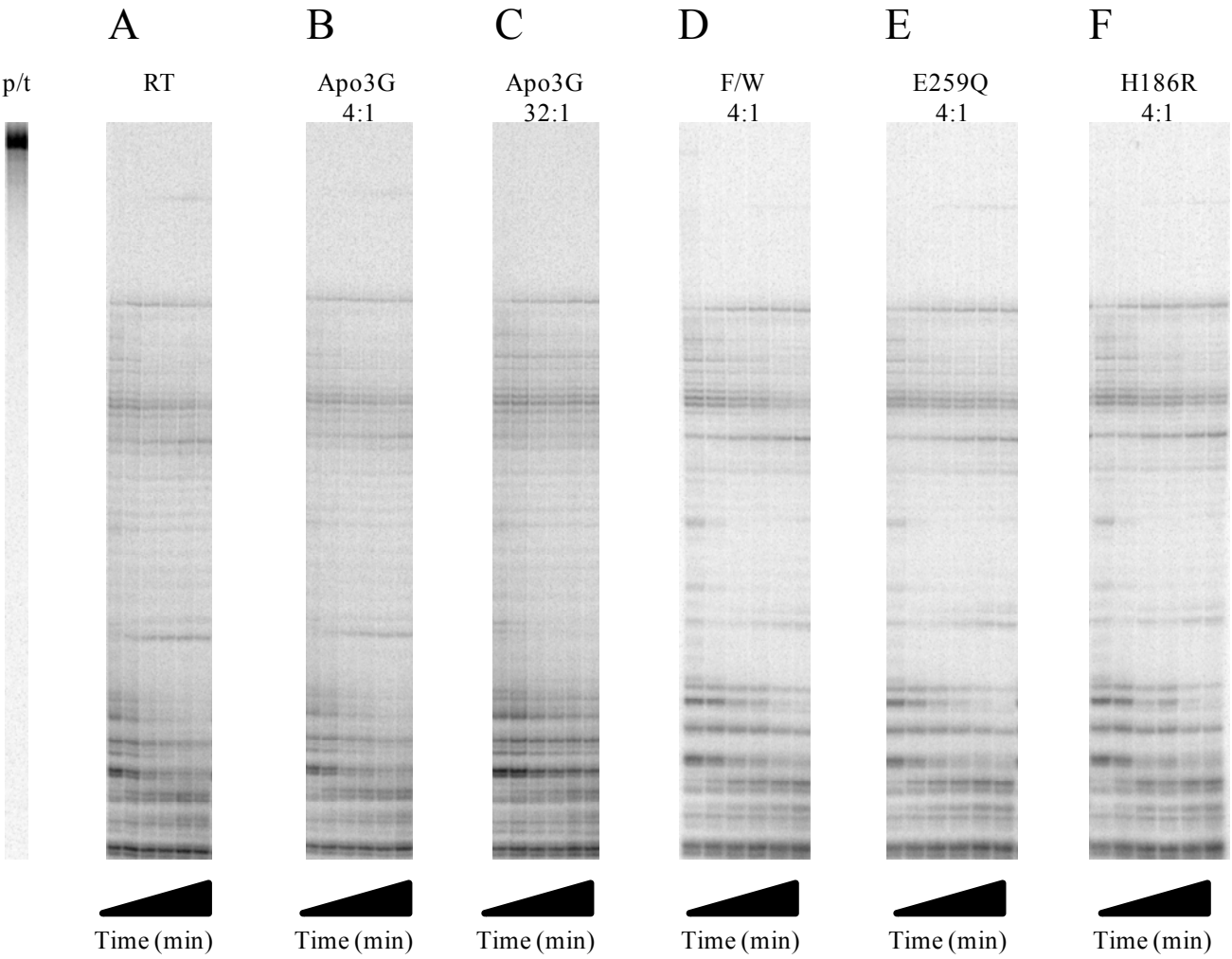

Figure 3.13 **The presence of APOBEC3G does not inhibit reverse transcriptase mediated RNAseH degradation of template RNA.** ^{32}-P labelled template RNA was heat annealed to a full complement of DNA to create a substrate for RNAseH. The substrate was added to reactions at 20 nM in the presence of RT buffer. Reactions contained 350 nM NC and 960 nM RT in the absence (A) or presence of Apo3G forms added at various ratios to the primer template: of native Apo3G, 4:1 (B), native Apo3G, 32:1 (C), F/W mutant, 4:1 (D), E259Q, 4:1 (E) or H186R, 4:1 (F). Samples were taken at 2.5, 5, 10, 15, 30 and 60 min. The single lane by itself (left), shows the unreacted primer template (p/t) as a negative control.

CHAPTER 4.O
DISCUSSION

4.1 Nucleocapsid-mediated annealing of $tRNA^{Lys,3}$ in the presence of APOBEC3G

Annealing of the $tRNA^{Lys,3}$ to the PBS region is the first important step of reverse transcription. RT needs the $tRNA^{Lys,3}$ to be annealed to the PBS region as the $tRNA^{Lys,3}$ functions as a primer that RT recognizes as a start site to begin reverse transcribing. This first step of reverse transcription is a logical place to begin investigating whether or not it is here that the deamination independent mechanism of Apo3G occurs, because if it did, it would impact reverse transcription events downstream of it. However, as evidenced by our annealing assays, the presence of Apo3G appears to not be able to inhibit NC-mediated strand annealing at low (4:1) or high (32:1) ratios of Apo3G to the primer/template (Figure 3.1). After titrating the concentration of NC down from an excess to determine the lowest level that allows NC mediated strand annealing to occur (Figure 3.2), we still see that neither Apo3G, nor any of the Apo3G mutants are able to inhibit NC mediated strand annealing (Figure 3.3). Furthermore, strand annealing reactions were set up with Apo3G prebound to the substrate to give Apo3G an "advantage" however, according to rotational anisotropy data (Table 3.1), this step is inconsequential as pre-binding the RNA with Apo3G appeared to not have an effect on the apparent K_d of NC. Similar to native Apo3G, both the monomeric F/W mutant and the catalytic mutant E259Q were unable to cause any discernible decrease in strand annealing (Figure 3.3). Accordingly, prebinding of Apo3G to RNA was unable to cause significant change in the affinity of NC for the RNA (Table 3.1). This suggests that although Apo3G and NC have similar binding affinities for the template RNA (Table 2, K_d of 402 and 383 nM, respectively), neither can compete the other off of the RNA substrate.

This agrees with Iwatani et al., who also show that the addition of Apo3G has no impact on NC mediated $tRNA^{Lys,3}$ annealing (Iwatani et al., 2007). Contrary to these findings Guo et al. provide evidence that Apo3G can inhibit NC mediated strand annealing (Guo et al., 2007). Guo and colleagues show that this occurs only at particular concentrations of Apo3G and NC that may not accurately reflect the ratios of these proteins to the $tRNA^{Lys,3}$ and RNA that is found *in vivo* (Guo et al., 2007). The assay we used however only detects changes in annealing as a function of a change in band migration. The annealing assay however does not detect whether or not the $tRNA^{Lys,3}$ is completely or partially annealed, which at the 3' of the $tRNA^{Lys,3}$ would obviously have an impact on primer extension initiation if it was not completely annealed.

4.2 Inhibition of reverse transcriptase-mediated primer extension by APOBEC3G is dependent on the ability of APOBEC3G to oligomerize and bind RNA with a high affinity

After the $tRNA^{Lys,3}$ has been annealed to PBS region, the next step of HIV reverse transcription is for RT to initiate primer extension. As Apo3G can bind to ssRNA, it was logical to hypothesize that it could bind to the PBS region of RNA and physically block RT from reverse transcribing, and therefore inhibit primer extension. Any changes in RT mediated primer extension with Apo3G present therefore could be attributed any of several of the predicted mechanisms of the deamination independent mode of Apo3G. The mechanisms that we chose to test were Apo3G oligomerization, the affinity of Apo3G for primer/template RNA, protein-protein interactions between RT and Apo3G and conformational changes of RNA caused by Apo3G.

We have shown that Apo3G can inhibit primer extension (Figure 3.4). We also investigated several mutant forms of Apo3G to elucidate a mechanism by which Apo3G could inhibit RT-mediated primer extension. The monomeric F/W mutant (Figure 3.5), the catalytic mutant E259Q (Figure 3.6), and the clinical mutant H186R (Figure 3.7) inhibited overall primer extension to the same extent as native Apo3G (Figure 3.4), but showed varying degrees of deficiency in attenuating production of the final extension product (Figure 3.8).

The data suggest that oligomeric versions of Apo3G that have a binding affinity for the RNA template which exceeds RT for an RNA template can partially block RT-mediated DNA synthesis (Table 3.2 and Figure 3.8). Data showing the deficiency of the monomeric F/W mutant in reverse transcriptase inhibition indicates that the ability to oligomerize on the RNA template appears to be the most important factor that enables inhibition of RT-mediated DNA synthesis (Figure 3.8). That oligomers of E259Q can bind RNA with a similar affinity to the F/W mutant (Table 3.2), but inhibit the formation of reverse transcripts with a median effectiveness in comparison to the F/W mutant and native Apo3G (Figure 3.8), suggests that RNA binding affinity is involved in the mechanism, although second in significance to oligomerization.

This suggests that the higher-order structures of Apo3G on RNA may act as a physical block. This is in contrast to a previous mechanism suggested for the deamination-independent mode of inhibition byApo3G that hypothesized that RNA binding ability alone was sufficient (Iwatani et al., 2007). Here we find that the mechanism is not only based on RNA binding, but also in what form the enzyme binds the template. Monomers of the F/W mutant and oligomers of E259Q, which have the similar binding affinity for the template (Table 3.2), have differential abilities to inhibit DNA synthesis

by RT (Figure 3.5, Figure 3.6 and Figure 3.8). Since Apo3G does not block RT from binding the primer/template (Figure 3.9), then RT would presumably have to displace Apo3G from the template to continue primer elongation. Accordingly, the data predict that Apo3G monomers can be displaced more easily by RT than Apo3G oligomers. In support of this prediction, the F/W mutant has been found to exhibit a 3-fold faster off-rate from ssDNA than native Apo3G (Chelico et al., 2010).

Another prediction of a model in which RT must displace Apo3G to extend the primer is that protein-protein interactions between RT and Apo3G do not play a role. Using a fluorescein labeled Apo3G (F-Apo3G), we found that Apo3G can interact with F-Apo3G with low affinity (K_d 3.5 μM, Figure 3.10). RT also binds to F-Apo3G with a low affinity (K_d 4 μM, Figure 3.10). All together these data demonstrate that protein-protein interactions between RT and Apo3G in solution are unfavourable. It is therefore likely that Apo3G does not inhibit primer extension by binding to RT *in vivo.*

It is also not likely that Apo3G mediates conformational changes in RNA that enable it to better inhibit primer extension. We see that only the F/W mutant is able to cause a significant change in RNA conformation (Figure 3.11). As F126A/W127A inhibited primer extension the least (Figure 3.8), the data suggest that conformational changes in RNA likely have little bearing on native Apo3G's ability to inhibit primer extension.

However using the same reasoning that oligomerization is important for inhibiting the production of final extension products, perhaps taking away the ability for Apo3G to oligomerize, as in the case of the F126A/W127A oligomerization mutant, allows Apo3G to cause a conformational change in the substrate RNA. This could result in a RNA conformation that is more conducive to reverse transcription, therefore giving RT a better substrate to reverse transcribe which may explain in part why the F126A/W127A mutant does not inhibit the formation of final extension as well as native Apo3G.

A study by Iwantani et al. also assessed the ability of Apo3G to inhibit primer extension (Iwatani et al., 2007). They found that Apo3G can inhibit RT mediated primer extension. However, the concentration of Apo3G relative to the primer/template used in most experiments was 16-fold higher than the primer template concentration, which is far greater than ratios used in this research and those estimated to be found *in vivo* (Table 1.1). Further, the RT concentration was at an equimolar ratio to the primer/template which is very low compared to *in vivo* estimations (Table 1.1). This ultimately raised questions as to whether or not Apo3G could actually inhibit primer extension under conditions that more accurately reflect *in vivo* conditions. In our studies we not only show that Apo3G can inhibit primer extension, but also that Apo3G can inhibit RT mediated primer extension when it is present at a

concentration that more accurately reflects the *in vivo* concentrations of all of the reverse transcription components. In addition to this, we suggest a mechanism for this inhibition which is based on the ability of Apo3G to oligomerize and on the affinity Apo3G for the primer/template RNA.

4.3 The use of E259Q as a null deaminase mutant

Previous studies have shown that E259Q was unable to inhibit the formation of reverse transcripts thereby suggesting that deamination was required (Mbisa et al., 2007; Miyagi et al., 2007; Schumacher et al., 2008). Here we show that E259Q is not biochemically the same as native Apo3G. The E259Q mutation causes a 2.5-fold decrease in primer/template binding affinity (Table 3.2, native Apo3G K_d 192 nM; E259Q K_d 477 nM). Although nucleic acid binding of Apo3G is largely contained within CD1 (Chelico et al., 2010; Chen et al., 2008) , the mutation of Glu259 in the active site CD2 is expected to affect substrate binding (Table 3.2). That E259Q is not biochemically similar to native Apo3G prevents interpretation of the importance of deamination in HIV inhibition using this mutant alone. Even with the decreased ability of E259Q to bind RNA, we found that it could still inhibit formation of reverse transcripts although 7-fold less than native Apo3G (Figure 3.8). This is in agreement with Bishop *et al*. (Bishop et al., 2008) that found the E259Q mutant to inhibit reverse transcripts but to a lesser extent than native Apo3G.

4.4 RNAseH activity in the presence of APOBEC3G

Before RT can begin copying the (-) strand DNA into (+) strand DNA, it must first degrade the RNA that it used as a template for the (–) strand DNA synthesis. RT utilizes an RNAseH domain to degrade the (–) strand RNA that it recognizes in a DNA/RNA hybrid. Our hypothesis was that Apo3G would not be able to inhibit the RNAseH activity of RT because of a low affinity for binding DNA/RNA hybrids (Iwatani et al., 2006), unless we found that there were a strong protein-protein interaction between RT and Apo3G. As we did not find a strong protein-protein interaction between RT and Apo3G, we therefore did not expect Apo3G to inhibit RNAseH activity of RT (Figure 3.10). We chose to use RNAseH assays to assess whether or not this was the case. When we used a full DNA/RNA hybrid as the substrate for the RT RNAseH in our RNAseH assay, we found that neither native Apo3G nor any the Apo3G mutants interfered with RNAseH-mediated RNA degradation (Figure 3.13). However, when we assessed RNAseH activity in a primer/extension reaction (Figure

3.12), we found that RNAseH inhibition corresponded with inhibition of final extension product (Figure 3.12 and Figure 3.8). This is due to the fact that the RNA primer must first be extended to form the RNAseH substrate. For example, we observed more RNA degradation when the F/W mutant was used than with native Apo3G (Figure 3.12). As a result, it can be said that Apo3G can indirectly inhibit RNAseH degradation by limiting the rate of primer extension.

Our results pertaining to the ability of Apo3G to inhibit RNAseH activity of RT are similar to those of Iwatani et al. (Iwatani et al., 2007). Even though the ratio of Apo3G:RNA is much higher in assays from the Iwatani et al. paper compared to our assays, their conclusion was that Apo3G did not inhibit the RT mediated RNAseH degradation of their RNA/DNA hybrid (Iwatani et al., 2007).

Contrary to our results, the study of Li et al. concluded that Apo3G can inhibit the RNAseH activity of RT (Li et al., 2007). Here Li et al. used only an RNA primer heat annealed to the DNA construct which resulted in less degradation products when Apo3G was present than when it was absent (Li et al., 2007). They claim that Apo3G can therefore directly inhibit RNAseH activity. This is similar to our results (Figure 3.12) with a primer/template in which we observed a decrease in degradation products from RT alone when Apo3G is present (Figure 3.4), but we attribute this to an indirect effect of Apo3G. The decrease in degradation products of RT are likely due to Apo3G's ability to inhibit primer extension (Figure 3.4*A-B*), and not direct RNAseH inhibition as when we use a full complement RNA/DNA hybrid, no degradation products are detected (Figure 3.13). This further confirms that Apo3G does not inhibit RNAseH activity, but merely inhibits the formation of the substrate RNA/DNA hybrid.

4.5 Overall Conclusion

Our data suggest a mechanism for how Apo3G can inhibit RT function. We show that this mechanism in not based upon the inhibition of NC mediated annealing of $tRNA^{Lys,3}$ to RNA or a direct inhibition of RNAseH activity of RT by Apo3G. We find that an important property of Apo3G contributing to the inhibition mechanism is its ability to oligomerize on nucleic acids (Chelico et al., 2010; Chelico et al., 2008) (Figure 3.5 and Figure 3.8) and bind RNA with high affinity (Table 3.1). The F/W mutant that has been found to be a monomer in solution and when bound to nucleic acids (Chelico et al., 2010; Huthoff et al., 2009), inhibits the synthesis of the final extension product of RT 20-fold less than native Apo3G at an enzyme:template ratio of 4:1 (Figure 3.8). Furthermore, our biochemical characterization of E259Q indicates that it should not be used interchangeably with native

Apo3G in experimental systems that require a deamination null mutant. The E259Q mutant inhibited final extension products of RT 7-fold less than native Apo3G (Figure 3.8). This is presumably because the binding affinity of E259Q for the primer/template is similar to that of RT but lower than that of native Apo3G (Table 3.2, K_d 477 nM, 529 nM and 192 nM, respectively) and RT can more effectively displace E259Q than native Apo3G. Our data suggests that oligomers of Apo3G may use the deamination-independent mode *in vivo* to inhibit or delay the formation of reverse transcripts, which can negatively impact HIV replication. Ascribing a mechanism to this mode of inhibition by Apo3G demonstrates that it could act in concert with deamination to inhibit HIV *in vivo*.

As more evidence is gained that validates the existence of an Apo3G deamination independent mechanism of HIV inhibition, it will likely be discovered that increasing intracellular levels of Apo3G would prove beneficial. As we increased the levels of Apo3G from 80 nM to 640 nM we saw a decrease in the formation of total and final extension products (Figures 3.4 to 3.8). Strategies that aim to increase intracellular levels of Apo3G will likely take advantage of this principle. It is likely that we would see the level of HIV restriction, probably being inhibition of RT mediated primer extension as seen in this study *in vitro*, being directly proportionate to the amount of Apo3G being present intracellularly. Being that the level of inhibition of the deamination dependent mechanism is likely limited by the C<u>C</u> motifs, having an alternate mode of HIV inhibition makes sense. The potential for inhibition is therefore likely higher for the deamination independent mechanism than it is for the deamination dependent mechanism as, increasing the level of Apo3G would increase the deamination independent inhibition, supposedly reducing the efficiency of reverse transcription. Whereas increasing the intracellular levels of Apo3G would, as previously mentioned, likely reach a limit where raising the intracellular level of Apo3G is no longer effective by just its deamination dependent mechanism alone. Some studies claim that the experimental procedures used in cell culture, such as Apo3G plasmid over expression, is responsible for the observed Apo3G deamination dependent mechanism necessary (Bishop et al., 2008; Mbisa et al., 2007; Miyagi et al., 2007; Schumacher et al., 2008). Even if this is the case, the fact remains that increasing intracellular levels of Apo3G resulted in HIV inhibition, assuming that Apo3G was being expressed at levels higher than what is normally seen intracellularly, therefore validating the theory that HIV inhibition is directly proportionate to intracellular levels of Apo3G.

In this study we only tested the initial steps of reverse transcription, namely $tRNA^{Lys,3}$ annealing and primer extension and RNAseH activity. However the results of this study are likely applicable to subsequent steps of reverse transcription such as primer extension after the first and second strand

transfers and DNA elongation after both of these steps (Figure 1.2). As long as there is Apo3G available, it should be able to inhibit primer extension by binding to RNA or ssDNA and preventing RT from efficiently polymerizing. It is likely that Apo3G can inhibit primer extension during DNA elongation (Figure 1.2 *Step 6*) as Apo3G can bind to ssDNA, although with less affinity for than for ssRNA (Iwatani et al., 2006). Whether or not Apo3G can reduce RT mediated primer extension on a DNA/DNA primer/template as well as on an RNA/RNA primer/template however remains to be seen.

CHAPTER 5.0
FUTURE STUDIES

5.1 *In vivo* expression of native, F126A/W127A and E259Q APOBEC3G

It would be interesting to see how well the results of this *in vitro* study translate *in vivo*. We saw that Apo3G can inhibit primer extension and that this may be a result of the ability of Apo3G to oligomerize on RNA and also based on its affinity for the RNA primer/template. We also saw that the E259Q deamination mutant may not serve as an ideal null proxy, as it does not behave exactly like Apo3G as based on our assays, the ability of E259Q to inhibit the formation of final extension products (Figure 3.6), and the affinity of E259Q for the RNA primer template is less than that of Apo3G (Table 3.2). We also saw that the monomeric F/W mutant was also less able to prevent the formation of final extension products as well as native Apo3G in addition to having a lower affinity for the RNA primer/template (Figure 3.5 and Table 3.2). To assess whether or not the lack of oligomerization (monomeric F/W mutant) or decreased binding affinity for the primer/template (monomeric F/W mutant and E259Q deamination null mutant) are important for having a reduced capacity to inhibit the formation of final extension products I would design an experiment to express these proteins by a gene knock in. With choosing a cell line which expresses Apo3G, i.e., CEM cells, you could knock out the natively expressed Apo3G and knock in either E259Q Apo3G mutant or the F/W mutant. Everything else being the same, the only difference would be the mutant variant of Apo3G being expressed, and not the level that it is being expressed at, thereby avoiding the over expression problem that hampered many past studies cells (Miyagi et al., 2007; Schumacher et al., 2008). This method is more likely to give a realistic representation of native Apo3G cellular cycling, and probably allow expression to be more akin to the levels seen with native Apo3G being expressed. If any inhibition was seen with the E259Q deamination null mutant, it could likely be attributed to the Apo3G deamination independent mechanism, although it would likely be somewhat attenuated, as evidenced by data from our studies. As for the monomeric F/W mutant, any reduction in the ability to reduce HIV infectivity, likely by a reduced capacity to prevent the formation of, for example, completely reverse transcribed reverse transcripts in quantities similar to when native Apo3G is used, could be attributed to the lack of the ability to oligomerize.

5.2 Implementing the $tRNA^{Lys,3}$ in primer extension assays

Instead of using a heat annealed primer for our primer extension assays, it would interesting to design an assay using the $tRNA^{Lys,3}$ annealed by NC. Although our data suggests that as Apo3G does

not inhibit NC mediated annealing of $tRNA^{Lys,3}$ to the PBS region, it would interesting to see if using the $tRNA^{Lys,3}$ would have result in any differences in primer extension. For example, perhaps the $tRNA^{Lys,3}$ is better able to recruit RT than the annealed RNA primer, resulting in a faster rate of primer initiation.

5.3 Assaying primer extension after the first and second strand transfers

Our assay only assessed whether or not Apo3G can inhibit primer extension of the PBS region. However there are multiple stages where the deamination independent mechanism of Apo3G can potentially impinge that we did not test. For example, after the first strand transfer and second strand transfer, RT must resume primer extension and DNA elongation. Using primer extension assays that model these events by using RNA or DNA templates that mimic these substrates would further verify the deamination independent mechanism of Apo3G. It is quite likely that if Apo3G inhibits RT at every stage of proviral DNA synthesis, that reducing the efficiency of primer extension at each of these steps would have an additive effect which would translate to a synergistic effect *in vivo*. Modest inhibition at multiple stages of reverse transcription would therefore likely have a big impact on the rate of formation of fully reverse transcribed proviral DNA ready to be integrated into the host genome. A significant reduction in the formation of provirus would therefore likely be seen, significantly restricting the HIV lifecycle.

CHAPTER 6.0
REFERENCES

An, P., Bleiber, G., Duggal, P., Nelson, G., May, M., Mangeat, B., Alobwede, I., Trono, D., Vlahov, D., Donfield, S.*, et al.* (2004). APOBEC3G Genetic Variants and Their Influence on the Progression to AIDS. Journal of Virology *78*, 11070-11076.

Arhel, N. (2010). Revisiting HIV-1 uncoating. Retrovirology *7*, 96.

Bampi, C., Jacquenet, S., Lener, D., Decimo, D., and Darlix, J.L. (2004). The chaperoning and assistance roles of the HIV-1 nucleocapsid protein in proviral DNA synthesis and maintenance. Int J Biochem Cell Biol *36*, 1668-1686.

Barat, C., Lullien, V., Schatz, O., Keith, G., Nugeyre, M.T., Gruninger-Leitch, F., Barre-Sinoussi, F., LeGrice, S.F., and Darlix, J.L. (1989). HIV-1 reverse transcriptase specifically interacts with the anticodon domain of its cognate primer tRNA. EMBO J *8*, 3279-3285.

Biasin, M., Piacentini, L., Caputo, S.L., Kanari, Y., Magri, G., Trabattoni, D., Naddeo, V., Lopalco, L., Clivio, A., Cesana, E.*, et al.* (2007). Apolipoprotein B mRNA-Editing Enzyme, Catalytic Polypeptide-Like 3G: A Possible Role in the Resistance to HIV of HIV-Exposed Seronegative Individuals. J Infect Dis *195*, 960-964.

Bishop, K.N., Holmes, R.K., and Malim, M.H. (2006). Antiviral potency of APOBEC proteins does not correlate with cytidine deamination. J Virol *80*, 8450-8458.

Bishop, K.N., Holmes, R.K., Sheehy, A.M., Davidson, N.O., Cho, S.J., and Malim, M.H. (2004). Cytidine deamination of retroviral DNA by diverse APOBEC proteins. Curr Biol *14*, 1392-1396.

Bishop, K.N., Verma, M., Kim, E.Y., Wolinsky, S.M., and Malim, M.H. (2008). APOBEC3G inhibits elongation of HIV-1 reverse transcripts. PLoS Pathog *4*, e1000231.

Bransteitter, R., Prochnow, C., and Chen, X.S. (2009). The current structural and functional understanding of APOBEC deaminases. Cell Mol Life Sci *66*, 3137-3147.

Briggs, J.A., Simon, M.N., Gross, I., Krausslich, H.G., Fuller, S.D., Vogt, V.M., and Johnson, M.C. (2004). The stoichiometry of Gag protein in HIV-1. Nat Struct Mol Biol *11*, 672-675.

Camaur, D., and Trono, D. (1996). Characterization of human immunodeficiency virus type 1 Vif particle incorporation. J Virol *70*, 6106-6111.

Chelico, L., Pham, P., Calabrese, P., and Goodman, M.F. (2006). APOBEC3G DNA deaminase acts processively 3' --> 5' on single-stranded DNA. Nat Struct Mol Biol *13*, 392-399.

Chelico, L., Prochnow, C., Erie, D.A., Chen, X.S., and Goodman, M.F. (2010). A structural model for deoxycytidine deamination mechanisms of the HIV-1 inactivation enzyme APOBEC3G. J Biol Chem *doi: 10.1074/jbc.M110.107987*.

Chelico, L., Sacho, E.J., Erie, D.A., and Goodman, M.F. (2008). A model for oligomeric regulation of APOBEC3G cytosine deaminase-dependent restriction of HIV. J Biol Chem *283*, 13780-13791.

Chen, K.M., Harjes, E., Gross, P.J., Fahmy, A., Lu, Y., Shindo, K., Harris, R.S., and Matsuo, H.

(2008). Structure of the DNA deaminase domain of the HIV-1 restriction factor APOBEC3G. Nature *452*, 116-119.

Chiu, Y.L., and Greene, W.C. (2008). The APOBEC3 cytidine deaminases: an innate defensive network opposing exogenous retroviruses and endogenous retroelements. Annu Rev Immunol *26*, 317-353.

Chiu, Y.L., and Greene, W.C. (2009). APOBEC3G: an intracellular centurion. Philos Trans R Soc Lond B Biol Sci *364*, 689-703.

Chiu, Y.L., Witkowska, H.E., Hall, S.C., Santiago, M., Soros, V.B., Esnault, C., Heidmann, T., and Greene, W.C. (2006). High-molecular-mass APOBEC3G complexes restrict Alu retrotransposition. Proc Natl Acad Sci U S A *103*, 15588-15593.

Coffin, J.M., Hughes, S.H.,Varmus, H.E. (1997). Retroviruses (Plainview (NY), Cold Spring Harbor Laboratory Press).

Douaisi, M., Dussart, S., Courcoul, M., Bessou, G., Vigne, R., and Decroly, E. (2004). HIV-1 and MLV Gag proteins are sufficient to recruit APOBEC3G into virus-like particles. Biochem Biophys Res Commun *321*, 566-573.

Feng, Y., and Chelico, L. (2011). Intensity of deoxycytidine deamination of HIV-1 proviral DNA by the retroviral restriction factor APOBEC3G is mediated by the non-catalytic domain. J Biol Chem.

Friedrich, B.M., Dziuba, N., Li, G., Endsley, M.A., Murray, J.L., and Ferguson, M.R. (2011). Host factors mediating HIV-1 replication. Virus Research *161*, 101-114.

Gallois-Montbrun, S., Kramer, B., Swanson, C.M., Byers, H., Lynham, S., Ward, M., and Malim, M.H. (2006). The antiviral protein APOBEC3G localizes to ribonucleoprotein complexes found in P-bodies and stress granules. J Virol.

Gao, F., Robertson, D.L., Morrison, S.G., Hui, H., Craig, S., Decker, J., Fultz, P.N., Girard, M., Shaw, G.M., Hahn, B.H.*, et al.* (1996). The heterosexual human immunodeficiency virus type 1 epidemic in Thailand is caused by an intersubtype (A/E) recombinant of African origin. Journal of Virology *70*, 7013-7029.

Gorry, P., and Ancuta, P. (2011). Coreceptors and HIV-1 Pathogenesis. Current HIV/AIDS Reports *8*, 45-53.

Grohmann, D., Godet, J., Mély, Y., Darlix, J.-L., and Restle, T. (2008). HIV-1 Nucleocapsid Traps Reverse Transcriptase on Nucleic Acid Substrates†. Biochemistry *47*, 12230-12240.

Guo, F., Cen, S., Niu, M., Saadatmand, J., and Kleiman, L. (2006). Inhibition of formula-primed reverse transcription by human APOBEC3G during human immunodeficiency virus type 1 replication. J Virol *80*, 11710-11722.

Guo, F., Cen, S., Niu, M., Yang, Y., Gorelick, R.J., and Kleiman, L. (2007). The interaction of APOBEC3G with human immunodeficiency virus type 1 nucleocapsid inhibits tRNA3Lys annealing to

viral RNA. J Virol *81*, 11322-11331.

Han, S., Marinova, E., and Zheng, B. (2004). Rectification of age-related impairment in Ig gene hypermutation during a memory response. Int Immunol *16*, 525-532.

Harris, R.S., and Liddament, M.T. (2004). Retroviral restriction by APOBEC proteins. Nat Rev Immunol *4*, 868-877.

Huthoff, H., Autore, F., Gallois-Montbrun, S., Fraternali, F., and Malim, M.H. (2009). RNA-dependent oligomerization of APOBEC3G is required for restriction of HIV-1. PLoS Pathog *5*, e1000330.

Iwatani, Y., Chan, D.S., Wang, F., Maynard, K.S., Sugiura, W., Gronenborn, A.M., Rouzina, I., Williams, M.C., Musier-Forsyth, K., and Levin, J.G. (2007). Deaminase-independent inhibition of HIV-1 reverse transcription by APOBEC3G. Nucleic Acids Res *35*, 7096-7108.

Iwatani, Y., Takeuchi, H., Strebel, K., and Levin, J.G. (2006). Biochemical activities of highly purified, catalytically active human APOBEC3G: correlation with antiviral effect. J Virol *80*, 5992-6002.

Kao, S., Khan, M.A., Miyagi, E., Plishka, R., Buckler-White, A., and Strebel, K. (2003). The human immunodeficiency virus type 1 Vif protein reduces intracellular expression and inhibits packaging of APOBEC3G (CEM15), a cellular inhibitor of virus infectivity. J Virol *77*, 11398-11407.

Knopp, R.H., Gitter, H., Truitt, T., Bays, H., Manion, C.V., Lipka, L.J., LeBeaut, A.P., Suresh, R., Yang, B., and Veltri, E.P. (2003). Effects of ezetimibe, a new cholesterol absorption inhibitor, on plasma lipids in patients with primary hypercholesterolemia. Eur Heart J *24*, 729-741.

Koning, F.A., Newman, E.N., Kim, E.Y., Kunstman, K.J., Wolinsky, S.M., and Malim, M.H. (2009). Defining APOBEC3 expression patterns in human tissues and hematopoietic cell subsets. J Virol *83*, 9474-9485.

Le Grice, S.F.J., and GrÜNinger-Leitch, F. (1990). Rapid purification of homodimer and heterodimer HIV-1 reverse transcriptase by metal chelate affinity chromatography. European Journal of Biochemistry *187*, 307-314.

Li, X.Y., Guo, F., Zhang, L., Kleiman, L., and Cen, S. (2007). APOBEC3G inhibits DNA strand transfer during HIV-1 reverse transcription. J Biol Chem *282*, 32065-32074.

Mangeat, B., Turelli, P., Caron, G., Friedli, M., Perrin, L., and Trono, D. (2003). Broad antiretroviral defence by human APOBEC3G through lethal editing of nascent reverse transcripts. Nature *424*, 99-103.

Mbisa, J.L., Barr, R., Thomas, J.A., Vandegraaff, N., Dorweiler, I.J., Svarovskaia, E.S., Brown, W.L., Mansky, L.M., Gorelick, R.J., Harris, R.S*., et al.* (2007). Human immunodeficiency virus type 1 cDNAs produced in the presence of APOBEC3G exhibit defects in plus-strand DNA transfer and integration. J Virol *81*, 7099-7110.

Miyagi, E., Opi, S., Takeuchi, H., Khan, M., Goila-Gaur, R., Kao, S., and Strebel, K. (2007). Enzymatically active APOBEC3G is required for efficient inhibition of human immunodeficiency virus

type 1. J Virol *81*, 13346-13353.

Newman, E.N., Holmes, R.K., Craig, H.M., Klein, K.C., Lingappa, J.R., Malim, M.H., and Sheehy, A.M. (2005). Antiviral function of APOBEC3G can be dissociated from cytidine deaminase activity. Curr Biol *15*, 166-170.

Patel, S.R., Harris, R.S., and Malhotra, A. (2002). Pulmonary dead space and survival. N Engl J Med *347*, 850-852; author reply 850-852.

Pillai, S.K., Wong, J.K., and Barbour, J.D. (2008). Turning up the volume on mutational pressure: is more of a good thing always better? (A case study of HIV-1 Vif and APOBEC3). Retrovirology *5*, 26.

Refsland, E.W., Stenglein, M.D., Shindo, K., Albin, J.S., Brown, W.L., and Harris, R.S. (2010). Quantitative profiling of the full APOBEC3 mRNA repertoire in lymphocytes and tissues: implications for HIV-1 restriction. Nucleic Acids Res.

Rein, A., Henderson, L.E., and Levin, J.G. (1998). Nucleic-acid-chaperone activity of retroviral nucleocapsid proteins: significance for viral replication. Trends Biochem Sci *23*, 297-301.

Santa-Marta, M., da Silva, F.A., Fonseca, A.M., and Goncalves, J. (2005). HIV-1 Vif can directly inhibit apolipoprotein B mRNA-editing enzyme catalytic polypeptide-like 3G-mediated cytidine deamination by using a single amino acid interaction and without protein degradation. J Biol Chem *280*, 8765-8775.

Sawyer, S.L., Emerman, M., and Malik, H.S. (2004). Ancient adaptive evolution of the primate antiviral DNA-editing enzyme APOBEC3G. PLoS Biol *2*, E275.

Schumacher, A.J., Hache, G., Macduff, D.A., Brown, W.L., and Harris, R.S. (2008). The DNA deaminase activity of human APOBEC3G is required for Ty1, MusD, and human immunodeficiency virus type 1 restriction. J Virol *82*, 2652-2660.

Sheehy, A.M., Gaddis, N.C., Choi, J.D., and Malim, M.H. (2002). Isolation of a human gene that inhibits HIV-1 infection and is suppressed by the viral Vif protein. Nature *418*, 646-650.

Soros, V.B., Yonemoto, W., and Greene, W.C. (2007). Newly Synthesized APOBEC3G Is Incorporated into HIV Virions, Inhibited by HIV RNA, and Subsequently Activated by RNase H. PLoS Pathog *3*, e15.

Stopak, K., de Noronha, C., Yonemoto, W., and Greene, W.C. (2003). HIV-1 Vif blocks the antiviral activity of APOBEC3G by impairing both its translation and intracellular stability. Mol Cell *12*, 591-601.

Strebel, K., and Khan, M.A. (2008). APOBEC3G encapsidation into HIV-1 virions: which RNA is it? Retrovirology *5*, 55.

Ulenga, N.K., Sarr, A.D., Hamel, D., Sankale, J.L., Mboup, S., and Kanki, P.J. (2008). The level of APOBEC3G (hA3G)-related G-to-A mutations does not correlate with viral load in HIV type 1-infected individuals. AIDS Res Hum Retroviruses *24*, 1285-1290.

Vazquez-Perez, J.A., Ormsby, C.E., Hernandez-Juan, R., Torres, K.J., and Reyes-Teran, G. (2009). APOBEC3G mRNA expression in exposed seronegative and early stage HIV infected individuals decreases with removal of exposure and with disease progression. Retrovirology *6*, 23.

Xu, H., Chertova, E., Chen, J., Ott, D.E., Roser, J.D., Hu, W.S., and Pathak, V.K. (2007). Stoichiometry of the antiviral protein APOBEC3G in HIV-1 virions. Virology *360*, 247-256.

Xu, X.M., Chen, Y., Chen, J., Yang, S., Gao, F., Underhill, C.B., Creswell, K., and Zhang, L. (2003). A peptide with three hyaluronan binding motifs inhibits tumor growth and induces apoptosis. Cancer Res *63*, 5685-5690.

Yu, X., Yu, Y., Liu, B., Luo, K., Kong, W., Mao, P., and Yu, X.F. (2003). Induction of APOBEC3G ubiquitination and degradation by an HIV-1 Vif-Cul5-SCF complex. Science *302*, 1056-1060.

Zennou, V., and Bieniasz, P.D. (2006). Comparative analysis of the antiretroviral activity of APOBEC3G and APOBEC3F from primates. Virology *349*, 31-40.

Zhang, H., Yang, B., Pomerantz, R.J., Zhang, C., Arunachalam, S.C., and Gao, L. (2003). The cytidine deaminase CEM15 induces hypermutation in newly synthesized HIV-1 DNA. Nature *424*, 94-98.

Zhu, P., Chertova, E., Bess, J., Jr., Lifson, J.D., Arthur, L.O., Liu, J., Taylor, K.A., and Roux, K.H. (2003a). Electron tomography analysis of envelope glycoprotein trimers on HIV and simian immunodeficiency virus virions. Proc Natl Acad Sci U S A *100*, 15812-15817.

Zhu, Y., Nonoyama, S., Morio, T., Muramatsu, M., Honjo, T., and Mizutani, S. (2003b). Type two hyper-IgM syndrome caused by mutation in activation-induced cytidine deaminase. J Med Dent Sci *50*, 41-46.